


Steered discrete-time quantum walks for engineering of quantum states

Gururaj Kadiri*

Materials Science Group, Indira Gandhi Centre for Atomic Research, Kalpakkam, Tamilnadu 603102, India

 (Received 24 May 2022; accepted 7 June 2023; published 7 July 2023)

We analyze the strengths and limitations of steered discrete-time quantum walks with position-independent coins in generating quantum states of bipartite quantum systems comprising of a qubit coupled to a qudit system. We demonstrate that not all quantum states in the composite space are accessible through such quantum walks, even under the most generalized definition of a quantum step, leading to a bifurcation of the composite Hilbert space into “walk-accessible states” and the “walk-inaccessible states.” We give an algorithm for generating any walk-accessible state from a simple-to-realize product state in a minimal number of walk steps, all of unit step size. We further give a prescription towards constructing minimal quantum walks between any pair of such walk-accessible states. Linear optics has been a popular physical system for implementing coin-based quantum walks, where the composite space is built up of spin and orbital angular momenta of light beams. We establish that in such an implementation, any generalized quantum step can be implemented up to a global phase using a single q -plate and a pair of homogeneous wave plates. We then give a quantum walk based scheme for realizing arbitrary vector beams consisting of a finite number of OAM components, using only q plates and wave plates.

DOI: [10.1103/PhysRevA.108.012607](https://doi.org/10.1103/PhysRevA.108.012607)

I. INTRODUCTION TO QUANTUM WALKS

The theory of classical random walks has been an indispensable tool to understand statistical phenomena and has been ubiquitous in modeling of various stochastic processes [1–5]. In one-dimensional random walks, the walker tosses a coin and moves forward or backward by one unit, depending upon the outcome of the toss. The quantum-mechanical counterpart of this are the discrete time quantum walks (DTQWs), where the walker and the coin obey the principles of quantum mechanics, and the motion of the walker and the toss of the coin are implemented as unitary transformations. Owing to quantum superposition effects, these walks display distinct statistical properties compared with their classical counterparts. Quantum walks have proved to be of immense utility in varied domains, like in quantum computation [6–8], quantum search [9], quantum algorithms [10,11], generating random numbers [12], modeling topological phenomena [13–17], etc. In the DTQWs, the walker is modeled as a qudit, belonging to a potentially infinite-dimensional space called the “walk space,” while the coin is modeled as a qubit, belonging to two-dimensional space called the “coin space.” In this context, another application of such quantum walks explored in recent years has been quantum state engineering (QSE) of high-dimensional quantum systems, which refers to constructing a desired quantum state starting from some simple-to-realize initial state. QSE is realized using DTQWs by carefully steering the quantum walk towards a certain state in the composite space and then projecting out the coin, such that the walker collapses into the desired state on the walk space [18–22]. Such high-dimensional states have myriad applications, since,

in general more can be accomplished in a qudit quantum system than in a qubit quantum system [23–25]. For instance, qudits are shown to be more powerful than qubits in tests exploring the foundations of quantum theory [26–28], in quantum machine learning [29], etc. In quantum cryptography, such states are shown to be more resilient to noise and also offer a larger secret key rate [30–34].

Quantum walks have been implemented in various physical systems [35]: NMR systems [36,37], on ion traps [38,39], in circuit QED [40] in neutral atoms [41], to name a few. In addition to these, photonic systems have also proved to be a very viable platform for implementing DTQWs, in that they have been demonstrated under various settings like, time-bin encoding [42], interferometers [43,44], and spin angular momentum and orbital angular momentum (SAM-OAM) of light beams [45–47].

In this paper, we examine the viability of DTQWs involving position-independent but time-dependent coins, in engineering of the quantum states of the composite space. In SAM-OAM optical implementation of the quantum walks, these states physically correspond to what are called vector beams, which are light beams having spatially varying polarization distribution across their transverse planes. Such vector light beams have found numerous applications in varied fields [48–53]. In this paper, we recast the above-mentioned “QSE using DTQWs” formulation as a means of generating desired vector vortex beams starting from standard Gaussian light beams.

The paper is organized as follows: In Sec. II, we give theoretical background of the DTQWs, and then present mathematical formulation of QSE in DTQWs. Section III is devoted towards defining a generalized quantum step, characterizing walks comprised of such quantum steps and the quantum states realized by such quantum walks. In Sec. IV,

*gururaj@igcar.gov.in

we present a deterministic recursive algorithm for generating walk-accessible composite states, starting from some easy-to-generate product states. In Sec. V, we introduce the notion of simplification of a quantum walk. We establish that given a quantum walk it is possible to construct another “simplified” quantum walk that is completely equivalent to it, but consisting of quantum steps of identical step size. Given a pair of walk-accessible states, we also provide here method for obtaining a “minimal quantum walk” that transforms one to the other. As a practical implementation of these ideas, in Sec. VI, we provide the implementation details for these targeted quantum walks in the linear optics domain. In Sec. VII we provide some numerical examples for the algorithms derived in the previous sections. In Sec. VIII, we conclude the paper by summarizing the results.

II. THEORETICAL BACKGROUND

For carrying out a DTQW, we identify a quantum system with two different degrees of freedom (DoFs): a qubit DoF called the “coin space” spanning the Hilbert space H_c and a qudit DOF called the “walk space” whose states belong to a Hilbert space H_w . An arbitrary state $|c\rangle \in H_c$ in the standard basis is given by

$$|c\rangle = c_0|\mathbf{0}\rangle + c_1|\mathbf{1}\rangle, \quad (1)$$

where c_0 and c_1 are complex numbers. We associate with every state $|c_\perp\rangle$ a unique state $|\bar{c}_\perp\rangle$ which is orthogonal to $|c\rangle$ defined in terms of components of $|c\rangle$ in the standard basis as

$$|\bar{c}_\perp\rangle = -\bar{c}_1|\mathbf{0}\rangle + \bar{c}_0|\mathbf{1}\rangle, \quad (2)$$

where the overbar indicates complex conjugation. Any state orthogonal to $|c\rangle$ will differ $|\bar{c}_\perp\rangle$ only by an overall phase factor. It is to be noted that $|\bar{c}_\perp\rangle$, the orthogonal state of $|c\rangle$, is not $|c\rangle$ but $-|c\rangle$. We use the symbol $|c; m\rangle$ to represent the product state $|c\rangle \otimes |m\rangle$, where $|c\rangle$ is a unit vector in H_c , m is an integer, and $|m\rangle$ is the m^{th} standard basis vector in H_w .

An arbitrary pure state in the composite space $H_c \otimes H_w$ is given by [54,55]

$$|P\rangle = \sum_{m=b}^{m=e} p_m |p_m; m\rangle, \quad (3)$$

where $|p_m\rangle$ are unit vectors in the coin space H_c , and p_m are non-negative real numbers. Given a composite state of the form Eq. (3), we define the integer interval $[b, e]$ as its “position span,” by which we mean that the probability amplitudes at all positions greater than e or less than b are all zero.

A. Coin-based quantum walks

A single step of the quantum walk is a product of these two operators:

$$\hat{T} = \hat{S}(\hat{C} \otimes \hat{I}_w), \quad (4)$$

where \hat{C} is an SU(2) operator called the “coin toss operator”:

$$\hat{C}(\alpha, \beta, \gamma) = \begin{pmatrix} e^{i\alpha} \cos \beta & -e^{-i\gamma} \sin \beta \\ e^{i\gamma} \sin \beta & e^{-i\alpha} \cos \beta \end{pmatrix} \quad (5)$$

in the $\{|\mathbf{0}\rangle, |\mathbf{1}\rangle\}$ basis of the coin space. The shift operator is given by

$$\hat{S} = \sum_m (|\mathbf{0}; m-1\rangle\langle\mathbf{0}; m| + |\mathbf{1}; m+1\rangle\langle\mathbf{1}; m|). \quad (6)$$

The initial state; that is, the state at the beginning of the quantum walk, is generally taken to be at position $m=0$ in some arbitrary coin state $|s\rangle$. A time-independent quantum walk constitutes of N such steps starting from this initial state, and it leads to a composite state of the form Eq. (3):

$$\hat{T}^N |s; 0\rangle = |W\rangle. \quad (7)$$

The state on the right-hand side (RHS) $|W\rangle$ is a composite state of the form Eq. (3). The role of coin operator leading to different composite states is studied in Ref. [56].

B. Quantum state engineering using quantum walks

We refer to the product state located at the position 0, that is states of the form $|u; 0\rangle$, as the “home states.” The problem of quantum state engineering is to generate a composite state, like Eq. (3), starting from some home state.

In this paper, we intend to address some of the following questions: (i) can all quantum states on the composite space; that is, states of the form Eq. (3), be generated by a quantum walk of the form Eq. (7) or some reasonable generalization of it, starting from some home state? (ii) If two composite states can be generated by quantum walks, can those two be connected by a quantum walk? (iii) If the answer to the previous question is in affirmative, can a minimal walk be found that accomplishes it in least number of unit-sized steps?

In this paper, we represent the quantum states as bold letters enclosed in the ket symbol. States belonging to the coin space H_c are represented by lowercase letters as in Eq. (1), while those belonging to the composite space $H_c \otimes H_w$ are represented by the uppercase letters as in the left-hand side of Eq. (3).

III. GENERALIZED COIN-BASED QUANTUM WALKS

Speaking of generalizing the quantum walks, one method has been to employ different coin operator at each step, so that in place of Eq. (7), we have

$$\hat{T}_N \cdots \hat{T}_1 |s; 0\rangle = |W\rangle, \quad (8)$$

where \hat{T}_i represents the i^{th} quantum step, differing in their coin-flip operators, Eq. (5). This is referred to as a quantum walk using a time-dependent coin. Another generalization of Eq. (7) has been to have different step sizes for forward and backward motion. For instance, in Refs. [18,19,57,58], the conditional shift operator employed was the one of moving forward or staying still, depending upon the state of the coin. Owing to the translational symmetry of the problem, this shift operator was shown to be equivalent to the standard shift operator, in the sense that the resulting composite states in the both cases are identical, up to a relabeling of the position states.

It is to be noted that replacing an SU(2) coin with a unitary one will not give access to any different set of states: a composite state accessible with a unitary coin is also accessible

with an SU(2) coin. Therefore in the rest of the paper, we shall restrict our attention to only SU(2) coins. Furthermore, there are generalizations of the discrete time quantum walks where the coins are position-dependent [22,59,60] or history-dependent [61–63]. Such treatment are also beyond the scope of this paper, as we intend to consider only those systems which can be readily implemented in the linear optics setting.

A. Generalized quantum steps

A single step of the quantum walk is an SU(2) operator \hat{T} on the composite system $H_c \otimes H_w$ of the form

$$\hat{T}_\Gamma(\delta, p, s, \mathbf{c}) = \hat{S}_\Gamma(\delta, p, s)[\hat{C}(s, \mathbf{c}) \otimes I_w], \quad (9)$$

where $\hat{C}(s, \mathbf{c})$ and $\hat{S}_\Gamma(\delta, p, s)$ are given by

$$\begin{aligned} \hat{C}(s, \mathbf{c}) &= |s\rangle\langle\mathbf{c}| + |s_\perp\rangle\langle\mathbf{c}_\perp|, \\ \hat{S}_\Gamma(\delta, p, s) &= \cos \frac{\Gamma}{2} I_c \otimes I_w + \sin \frac{\Gamma}{2} \sum_m (e^{i\delta} |s_\perp; m+p\rangle\langle s; m| \\ &\quad - e^{-i\delta} |s; m-p\rangle\langle s_\perp; m|), \end{aligned} \quad (10)$$

where Γ and δ are real numbers between 0 and 2π , d is a nonzero integer and I_c and I_w are identity operators in the coin and walk space respectively. The coin operator $\hat{C}(s, \mathbf{c})$ is completely equivalent to the coin operator $\hat{C}(\alpha, \beta, \gamma)$ defined in Eq. (5), only parametrized differently. Here we have parametrized it by two unit vectors \mathbf{c} and s of the coin space. The action of coin-toss operator $\hat{C}(s, \mathbf{c})$ is to unitarily transform the orthogonal pair of states $|\mathbf{c}\rangle$ and $|\mathbf{c}_\perp\rangle$ to another orthogonal pair of states $|s\rangle$ and $|s_\perp\rangle$, respectively. The shift operator $\hat{S}_\Gamma(\delta, d, s)$ leaves a fraction of the state unaltered, and with the remaining fraction, it moves forward in the position space by p units if the coin state is $|s\rangle$, and moves backwards by the same number of units if the coin state is $|s_\perp\rangle$. Simultaneously, it also transforms the coin states $|s\rangle$ and $|s_\perp\rangle$ into $e^{i\delta}|s_\perp\rangle$ and $-e^{-i\delta}|s\rangle$, respectively. The action of $\hat{T}_\Gamma(\delta, p, s, \mathbf{c})$ on the orthogonal states $|\mathbf{c}; m\rangle$ and $|\mathbf{c}_\perp; m\rangle$ is given by

$$\begin{aligned} \hat{T}_\Gamma(\delta, p, s, \mathbf{c})|\mathbf{c}; m\rangle &= \cos \frac{\Gamma}{2} |s; m\rangle + \sin \frac{\Gamma}{2} e^{i\delta} |s_\perp; m+p\rangle, \\ \hat{T}_\Gamma(\delta, p, s, \mathbf{c})|\mathbf{c}_\perp; m\rangle &= \cos \frac{\Gamma}{2} |s_\perp; m\rangle - \sin \frac{\Gamma}{2} e^{-i\delta} |s; m-p\rangle. \end{aligned} \quad (11)$$

We shall regard Eq. (11) as the definition of the quantum step $\hat{T}_\Gamma(\delta, p, s, \mathbf{c})$, being completely equivalent to Eq. (10). The action of $\hat{T}_\Gamma(\delta, p, s, \mathbf{c})$ on any other product state $|\mathbf{w}; m\rangle$ can be obtained by expressing $|\mathbf{w}\rangle$ in the basis $(|\mathbf{c}\rangle, |\mathbf{c}_\perp\rangle)$ and acting it linearly on them. Its action on an arbitrary composite state can be found by acting it on each of the constituent terms. In the quantum step $\hat{T}_\Gamma(\delta, p, s, \mathbf{c})$, we call the state $|\mathbf{c}\rangle$ as its coin state and $|s\rangle$ as its shift state. Here p is an integer, indicating the size of the step. This quantum step is called position-independent or translationally invariant, because the parameters of the step are independent of the position m on which it is acting. The presence of Γ makes the quantum step very different from that of Eq. (4) as only a fraction of the state now undergoes the quantum walk, with Γ determining that fraction: $\Gamma = \pi$ leading to complete state transfer, while $\Gamma = 0$ corresponds to no change in the walk space.

Such walks have been termed “hybrid walks” in literature [64]. While Γ can range from $[0, 4\pi)$, it is easy to see that $\hat{T}_\Gamma(\delta, p, s, \mathbf{c}) = \hat{T}_{4\pi-\Gamma}(\pi + \delta, p, s, \mathbf{c})$ and therefore Γ can be restricted to $[0, 2\pi]$. The quantum steps $\hat{T}_0(\cdot, \cdot, s, \mathbf{c})$, i.e., the steps with $\Gamma = 0$ refer only to SU(2) transformation from \mathbf{c} to s , acting only on the coin space:

$$\hat{T}_0(\cdot, \cdot, s, \mathbf{c}) = \hat{C}(s, \mathbf{c}) \otimes I_w, \quad (12)$$

where $\hat{C}(s, \mathbf{c})$ is the operator defined in the first of Eq. (10). The step size p and the relative phase δ in this case are immaterial, and hence they are suppressed in Eq. (12). We call these steps as the “improper steps,” as against the steps with $\Gamma > 0$ and $p \neq 0$, which we call as the “proper steps.”

The quantum step Eq. (11) is such that, in one proper step at most only two other states, at a fixed distance ($\pm p$) from the current state, are accessed. We shall regard the step defined in Eq. (11) as the most generalized quantum walk step. This claim requires some justification, since we still have the same step size p in both forward and backward directions. This definition of a quantum step is the most general, in the sense that any further relaxation in the definition will be inconsistent with the requirement of translational invariance. It is essential, for instance, that the coin states at the m^{th} and $(m \pm p)^{\text{th}}$ positions appearing in the right-hand side of Eq. (11) be orthogonal to each other. Likewise, having distinct step sizes in the forward and backward directions is not consistent with translational invariance, unless Γ is fixed to π . In this paper, we have made a choice to force identical step size in the forward and backward directions, retaining the facility to have a variable Γ instead, a choice motivated by the linear optics implementation, to be introduced in Sec. VI. It must be noted that the second relation in Eq. (11) is not independent, but follows directly from the first, by requiring that \hat{T} act as an SU(2) operator in the composite space.

We represent a collection of M such steps by the symbol \hat{W} :

$$\hat{W} = \hat{T}_{\Gamma_M}(\delta_M, p_M, s_M, \mathbf{c}_M) \cdots \hat{T}_{\Gamma_1}(\delta_1, p_1, s_1, \mathbf{c}_1). \quad (13)$$

We call this sequence of steps \hat{W} as the “quantum walk.” The walk \hat{W} acts on the states from the left. We shall consider the dimension of walk space to be larger than $N = \max(|b|, |e|)$ of all the involved composite states, and also larger than $|p_1| + |p_2| + \cdots + |p_M|$ of all the involved steps.

B. Identifying states obtained by quantum walks

A quantum walk \hat{W} starting from an arbitrary home state $|\mathbf{u}; 0\rangle$ can be described as

$$\hat{W}|\mathbf{u}, 0\rangle = |\mathbf{U}\rangle \equiv \sum_{m=b}^{m=e} u_m |\mathbf{u}_m; m\rangle, \quad (14)$$

where the state $|\mathbf{U}\rangle$ on the RHS is a unit vector of the same form as the generic composite state $|\mathbf{P}\rangle$ of Eq. (3). We shall refer to such states, that is, composite states which are output of a quantum walk starting from some home state, as the walk accessible states, or simply “walk states.” We now derive a condition that distinguishes these walk states from the generic composite states of Eq. (3). From translation symmetry, if $\hat{W}|\mathbf{u}; 0\rangle = |\mathbf{U}\rangle$ then $\hat{W}|\mathbf{u}; d\rangle = |\mathbf{U}_{+d}\rangle$, where d is an integer

and $|\mathbf{U}_{+d}\rangle$ is $|\mathbf{U}\rangle$ shifted on the walk forward en masse by d units:

$$|\mathbf{U}_{+d}\rangle = \sum_{n=b}^{n=e} u_n |\mathbf{u}_n; n+d\rangle. \quad (15)$$

Since $|\mathbf{u}; 0\rangle$ and $|\mathbf{u}; d\rangle$ are orthogonal, and since the walk operator \hat{W} is a unitary operator, we demand the resulting states $|\mathbf{U}\rangle$ and $|\mathbf{U}_{+d}\rangle$ to also be orthogonal, $\langle \mathbf{U} | \mathbf{U}_{+d} \rangle = 0$, for all $d \neq 0$. The nontrivial d s being $d = 1, \dots, e - b$, leading to $e - b$ constraints:

$$\begin{aligned} \langle \mathbf{U} | \mathbf{U}_{+d} \rangle &= \sum_{m=b}^{m=e-d} u_m u_{m+d} \langle \mathbf{u}_m | \mathbf{u}_{m+d} \rangle = 0, \\ \forall d &= 1, \dots, e - b. \end{aligned} \quad (16)$$

This result indicates that not all composite states are walk states, only those which satisfy the constraints of Eq. (16) are. We shall refer to the walk-inaccessible composite states as the ‘‘non-walk states.’’ These states do not satisfy Eq. (16).

C. Generating new walk states from existing ones

It must be noted that a linear combination of two walk states need not be a walk state. The set of walk states, therefore do not form a subspace. This can be easily seen by noting that all the states belonging to the standard product basis $\{|\mathbf{0}\rangle, |\mathbf{1}\rangle\} \otimes \{\dots, |-\mathbf{1}\rangle, |\mathbf{0}\rangle, |\mathbf{1}\rangle, \dots\}$ are walk states, and therefore if the linear combination of walk states also yielded a walk state, then every state in the composite space would have been a walk state.

Given a walk state $|\mathbf{U}\rangle$ with position span $[b, e]$, one can generate another walk state $|\mathbf{U}_{+d}\rangle$ with span $[b+d, e+d]$ by shifting each position m in $|\mathbf{U}\rangle$ by d units as in Eq. (15). Likewise, we define another walk state $|\mathbf{U}_{\times d}\rangle$ as

$$|\mathbf{U}_{\times d}\rangle = \sum_{n=b}^{n=e} u_n |\mathbf{u}_n; nd\rangle. \quad (17)$$

It is easy to confirm that $|\mathbf{U}_{\times d}\rangle$ is also a walk state. If a walk \hat{W} generates $|\mathbf{U}\rangle$, then $|\mathbf{U}_{\times d}\rangle$ can be generated by changing the step size p_i of each step $\hat{T}_i(\delta_i, p_i, \mathbf{u}_i, \mathbf{c}_i)$ of \hat{W} by $p_i \times d$.

Recall that the action of a linear operator on an N -dimensional space gets fixed only by specifying its action on N linearly independent vectors. In case of the walk operator, however, once the action of \hat{W} on any state $|\mathbf{u}; 0\rangle$ is specified, as in Eq. (14), then its action on any other state, be it a home state, a product state, or a composite state, gets fixed, owing to its being SU(2) and translationally invariant. Particularly, between orthogonal home states we have the following relation:

$$\begin{aligned} \text{if } \hat{W}|\mathbf{u}; 0\rangle &= |\mathbf{U}\rangle, \\ \text{then } \hat{W}|\mathbf{u}_{\perp}; 0\rangle &= |\mathbf{U}_{\perp}\rangle, \end{aligned} \quad (18)$$

where, for a given $|\mathbf{U}\rangle$, the composite state $|\mathbf{U}_{\perp}\rangle$ is defined as

$$|\mathbf{U}_{\perp}\rangle = \sum_{m=-e}^{m=-b} u_{-m} |(\mathbf{u}_{-m})_{\perp}; m\rangle, \quad (19)$$

where $|(\mathbf{u}_{-m})_{\perp}\rangle$ is the state orthogonal to $|\mathbf{u}_{-m}\rangle$. It is easy to see that the walk states $|\mathbf{U}\rangle$ and $|\mathbf{U}_{\perp}\rangle$ are orthogonal to each other.

Therefore, given a walk state $|\mathbf{U}\rangle$, we can construct another walk state $|\mathbf{U}_{\perp}\rangle$, and two other families of walk states $|\mathbf{U}_{+d}\rangle$ and $|\mathbf{U}_{\times d}\rangle$ by shifting and scaling the walk position labels, respectively. Furthermore, any complex linear combination of the walk states $|\mathbf{U}\rangle$ and $|\mathbf{U}_{\perp}\rangle$ is also a legitimate walk state for any d . This facility enables us to construct new walk states of larger span from walk states of smaller span.

D. Characterizing the walk states

Given two walk states, we are interested in knowing whether they are a result of same walk \hat{W} , but with different home states or not. Let $|\mathbf{P}\rangle$ and $|\mathbf{Q}\rangle$ be the two walk states resulting from a quantum walk \hat{W} , from home with coin states $|\mathbf{p}\rangle$ and $|\mathbf{q}\rangle$ respectively. Owing to the SU(2) nature of the quantum walks, the necessary and also sufficient condition for this to hold can be derived to be

$$\begin{aligned} \text{if } |\mathbf{P}\rangle &= \hat{W}|\mathbf{p}; 0\rangle \quad \text{and} \quad |\mathbf{Q}\rangle = \hat{W}|\mathbf{q}; 0\rangle \quad \text{then} \\ |\langle \mathbf{P} | \mathbf{Q} \rangle|^2 &+ |\langle \mathbf{P} | \mathbf{Q}_{\perp} \rangle|^2 = 1. \end{aligned} \quad (20)$$

This result indicates that all composite states accessible by a given quantum walk (starting from different home states) reside in a two-dimensional subspace.

IV. SHRINKING ALGORITHM AND STEERED QUANTUM WALKS

It is to be noted that a quantum walk \hat{W} preserves the translational invariance of composite states: it takes walk states to walk states and non-walk states to non-walk states. Given a step $\hat{T}_i(\delta, p, s, \mathbf{c})$, we define its inverse $[\hat{T}_i(\delta, p, s, \mathbf{c})]^{-1}$ as the operator that undoes the action of $\hat{T}_i(\delta, p, s, \mathbf{c})$. The inverse of a quantum step is also a quantum step. It is easy to see that

$$[\hat{T}_i(\delta, p, s, \mathbf{c})]^{-1} = \hat{T}_i(\pi + \delta, p, \mathbf{c}, s). \quad (21)$$

Since each step of a walk is invertible, the walks themselves are invertible. So, given any walk state there always exist quantum walks that takes it to one of the home states. Inverting this walk would then yield a walk from a home state $|\mathbf{u}\rangle$ to the desired walk state $|\mathbf{U}\rangle$. Here we propose an algorithm to find a walk of $p = 1$ quantum steps that can convert the given walk state $|\mathbf{U}\rangle$ to a home state $|\mathbf{u}\rangle$. This is accomplished in just N number of $p = 1$ quantum steps, where $N = \max(|b|, |e|)$.

We start with the simplest case first: when the walk state is of a single term $|\mathbf{u}; m\rangle$. A quantum step $\hat{T}_\pi(0, 1, s, \mathbf{u}_{\perp})$ on $|\mathbf{u}; m\rangle$ yields $|\mathbf{s}; m-1\rangle$. Now, from here, taking $m-1$ steps of $\hat{T}_\pi(0, 1, s, \mathbf{s}_{\perp})$, we land on the home state $|\mathbf{s}; 0\rangle$:

$$|\mathbf{s}; 0\rangle = \hat{T}_\pi(0, 1, s, \mathbf{s}_{\perp})^{m-1} \hat{T}_\pi(0, 1, s, \mathbf{u}_{\perp}) |\mathbf{u}; m\rangle. \quad (22)$$

We now consider the case of reducing an arbitrary walk state $|\mathbf{U}\rangle$ to some home state $|\mathbf{u}; 0\rangle$. We achieve this using a recursive method: we find a walk step \hat{T}_1 , that can convert the given state $|\mathbf{U}\rangle$ of walk-spread $[b, e]$ into a composite beam $|\mathbf{U}_1\rangle$ of a shorter spread $[b+1, e-1]$. This is always possible if $|\mathbf{U}\rangle$ is a walk state, proof of which is given in the Appendix. One set of parameters of \hat{T}_1 that accomplishes this is given by (see

Appendix):

$$\begin{aligned} |c\rangle &= |\mathbf{u}_{e\perp}\rangle, \\ \Gamma &= 2 \tan^{-1} \left(\frac{u_e}{u_{e-1} |\langle \mathbf{u}_{e\perp} | \mathbf{u}_{e-1} \rangle|} \right), \\ \delta &= \pi - \Phi(\langle \mathbf{u}_{e\perp} | \mathbf{u}_{e-1} \rangle). \end{aligned} \quad (23)$$

Now, note that the ensuing state $|U_1\rangle$ is also a walk state, having obtained through a quantum step on a walk state. It can also be reduced to another composite state $|U_2\rangle$ whose spread is $[b+2, e-2]$, by using another walk step \hat{T}_2 , whose parameters can be computed in a similar manner as in Eq. (23). Proceeding this way for a total $(e-b)/2$ steps if b and e are of same parity, or for $(e-b+1)/2$ steps if they are of different parity, one lands in a separable state $|\mathbf{u}; p\rangle$, where p is equal to $(b+e)/2$ in the former case and $(b+e-1)/2$ in the latter case. Now, if $p=0$, we are at home, and therefore have accomplished what we have set out to. Otherwise, transform $|\mathbf{u}; p\rangle$ into $|s; 0\rangle$ in p steps as in Eq. (22). Therefore, in either case, in a total of $N = \max(|b|, |e|)$ steps it is possible to reduce a composite state of spread $[b, e]$ into a home state:

$$\hat{T}_N \cdots \hat{T}_2 \hat{T}_1 |U\rangle = |\mathbf{u}; 0\rangle. \quad (24)$$

We call this process as the ‘‘shrinking algorithm,’’ as the position span of the composite state shrinks after each step. Now, it follows from Eq. (24) that the composite state $|U\rangle$ can be constructed from the home state $|\mathbf{u}\rangle$ by taking the inverse of those N steps, in the opposite order:

$$|U\rangle = \hat{W}_{\min} |\mathbf{u}; 0\rangle, \quad (25)$$

where

$$\hat{W}_{\min} = \hat{T}_1^{-1} \cdots \hat{T}_N^{-1}, \quad (26)$$

with the inverse of a walk step \hat{T} defined in Eq. (21). This completes the algorithm to deterministically reach a given walk state from some home state. We call this the steered quantum walk algorithm. Note that the shift state $|s\rangle$ does not appear in the Eq. (23), implying that the shrinking algorithm is does not place any restriction on the shift state of any quantum step. Now, recall that the steps appearing in the steering quantum walk algorithm are the inverses of those appearing in the shrinking algorithm. Since the coin and step states of a step and its inverse are swapped [see Eq. (21)], the steered quantum walk algorithm is arbitrary up to the coin state of each of its steps.

V. SIMPLIFYING THE QUANTUM WALKS

A. Simplifying a quantum walk

In Sec. IV, given a walk state, an algorithm was prescribed for obtaining a walk and a home state which together generate the given walk state. Here we discuss a case where the walk \hat{W} of the form Eq. (13) is given instead of a walk state. Recall that our definition of the quantum walk allows it to be composed of steps of unequal step-sizes, different coin, shift states etc. Given such a walk, we intend to find another walk \hat{W}_{\min} , that functions like \hat{W} , but consisting steps of identical step-size $p=1$, and all with the same coin state $|c\rangle$.

Towards this, pick up an arbitrary home state $|\mathbf{p}; 0\rangle$. Let $|\mathbf{P}\rangle$ be the outcome of quantum walk \hat{W} starting with this home state. Now, ignoring \hat{W} , we could start from $|\mathbf{P}\rangle$ and, from the shrinking algorithm of Sec. IV, get a walk \hat{W}_s , and a home state $|\mathbf{p}_s\rangle$. Now, how are \hat{W}_s and \hat{W} related? Both lead to the same walk state, but for different home states $\hat{W}|\mathbf{p}\rangle = \hat{W}_s|\mathbf{p}_s\rangle$. They are only related by an SU(2) operation in the coin space:

$$\hat{W} = \hat{W}_s \hat{T}_0(\cdot, \cdot, \mathbf{p}_s, \mathbf{p}). \quad (27)$$

We say the walk on the RHS, $\hat{W}_s \hat{T}_0(\cdot, \cdot, \mathbf{p}_s, \mathbf{p})$, as the walk that ‘‘minimizes the walk \hat{W} ,’’ and represent it as $\mathbf{min}(\hat{W})$.

At this stage, it is important to note that it is always possible to absorb an improper step into a proper quantum step that follows it, as

$$\hat{T}_\Gamma(\delta, d, s, \mathbf{c}) \hat{T}_0(\cdot, \cdot, \mathbf{p}, \mathbf{q}) = \hat{T}_\Gamma(\delta, p, s, \mathbf{w}), \quad (28)$$

where the coin state $|\mathbf{w}\rangle$ of the step on the RHS is given by $|\mathbf{w}\rangle = \hat{T}_0^{-1}(\cdot, \cdot, \mathbf{p}, \mathbf{q})|c\rangle$.

The improper step $\hat{T}_0(\cdot, \cdot, \mathbf{p}_s, \mathbf{p})$ of Eq. (27) can be absorbed into the first step of \hat{W}_s , as in Eq. (28), so that the minimal walk $\mathbf{min}(\hat{W})$ contains only as many steps as are in \hat{W}_s .

B. Quantum walks between two walk states

While the paper until now discussed the cases of a quantum walk starting from home states to the composite walk states, in this section we discuss about going from one composite walk state to another composite walk state through a minimal quantum walk. That is, given two walk states $|\mathbf{P}\rangle$ and $|\mathbf{Q}\rangle$, we seek the minimal quantum walk \hat{W}_{\min} such that $|\mathbf{Q}\rangle = \hat{W}_{\min}|\mathbf{P}\rangle$. One way to generate \hat{W}_{\min} is to first obtain some walk \hat{W} that accomplishes this, and then get \hat{W}_{\min} as $\mathbf{min}(\hat{W})$, using the minimization method discussed above. One such walk \hat{W} that takes $|\mathbf{P}\rangle$ to $|\mathbf{Q}\rangle$ can be

$$\hat{W} = \hat{W}_Q \hat{T}_0(\cdot, \cdot, \mathbf{q}, \mathbf{p}) \hat{W}_P^{-1}, \quad (29)$$

where the walks \hat{W}_P and \hat{W}_Q are the minimal walks that take the walk states $|\mathbf{P}\rangle$ and $|\mathbf{Q}\rangle$ to the home states $|\mathbf{p}; 0\rangle$ and $|\mathbf{q}; 0\rangle$, respectively, and $\hat{T}_0(\cdot, \cdot, \mathbf{q}, \mathbf{p})$ is the improper step that takes $|\mathbf{p}\rangle$ to $|\mathbf{q}\rangle$ in the coin space:

$$\hat{W}_P |\mathbf{p}; 0\rangle = |\mathbf{P}\rangle,$$

$$\hat{W}_Q |\mathbf{q}; 0\rangle = |\mathbf{Q}\rangle,$$

$$\hat{T}_0(\cdot, \cdot, \mathbf{q}, \mathbf{p}) = (|\mathbf{q}\rangle \langle \mathbf{p}| + |\mathbf{q}_\perp\rangle \langle \mathbf{p}_\perp|) \otimes I_w.$$

The minimal quantum walk \hat{W}_{\min} to accomplish this can then be found by minimizing the above walk \hat{W} by the method discussed in Sec. VA.

VI. OPTICAL IMPLEMENTATION

We now provide a means of realizing the aforementioned ideas on an actual physical hardware over which such quantum walks are being implemented. In the linear optical implementation of DTQWs, the spin angular momentum (SAM) of the light beam as the coin space H_c , and its orbital angular momentum (OAM) acts as the walk space, H_w . The state of polarization (SoP) of a light beam characterizes the SAM of light, with left circular polarization identified with +1

units of SAM and right-circular polarization identified with -1 units of it. OAM, on the other hand, is independent of the SAM of the light beam and characterizes the helicity of its wave front. An arbitrary composite state of the light beam is the one which exists in a superposition of combinations of spin and orbital angular momenta, such that a definite SoP or OAM cannot be assigned to it. Such beams are termed vector beams, and they can be identified by the varying phase and SoP distribution across their transverse plane.

A. Scalar and vector beams

An arbitrary SoP of a light beam can be represented as a two-component unit vector, $|\mathbf{u}\rangle$ called the ‘‘Jones vector,’’ in some orthogonal basis, as in Eq. (1). For implementing the SoP as a coin space, we identify the states $|\mathbf{0}\rangle$ and $|\mathbf{1}\rangle$ with $|\mathbf{l}\rangle$ and $|\mathbf{r}\rangle$, the left and right circular polarization states of light, respectively. The states $|\mathbf{h}\rangle$, $|\mathbf{v}\rangle$, $|\mathbf{d}\rangle$, and $|\mathbf{a}\rangle$, defined following Eq. (41), will then correspond to horizontal, vertical, diagonal, and anti-diagonal SoPs of light, respectively. In the numerical simulations carried out in this work, the computational basis vectors $[1, 0]^T$ and $[0, 1]^T$ respectively stand for $|\mathbf{h}\rangle$ and $|\mathbf{v}\rangle$ states. The left- and right-circular SoPs $|\mathbf{l}\rangle$ and $|\mathbf{r}\rangle$ would then correspond to the column vectors $\frac{1}{\sqrt{2}}[1, i]^T$ and $\frac{1}{\sqrt{2}}[i, 1]^T$, respectively.

Unitary transformations between pairs of SoPs are affected using wave plates. In this paper, we represent them by the symbol $\hat{p}_\Gamma(\alpha)$, where Γ is its retardance, and α is the angle its fast axis makes with the x axis. The action of this wave plate on an arbitrary SoP $|\mathbf{u}\rangle$ is given by

$$\hat{p}_\Gamma(\alpha)|\mathbf{u}\rangle = -\sin\frac{\Gamma}{2}\langle\mathbf{r}|\mathbf{u}\rangle e^{-2i\alpha}|\mathbf{l}\rangle + \cos\frac{\Gamma}{2}|\mathbf{u}\rangle + \sin\frac{\Gamma}{2}\langle\mathbf{l}|\mathbf{u}\rangle e^{2i\alpha}|\mathbf{r}\rangle. \quad (30)$$

Here $\langle\mathbf{l}|\mathbf{u}\rangle$ and $\langle\mathbf{r}|\mathbf{u}\rangle$ stand for the left and right circular polarization components of $|\mathbf{u}\rangle$. It is important to note it is always possible to transform one SoP to another SoP ‘‘up to a phase’’ using a single wave plate, and even ‘‘including the phase’’ by using a three-plate gadget consisting of a half-wave plate inserted in between two quarter-wave plates ([65,66]).

A vector beam is a light beam whose SoP varies across its transverse plane. In this work, we shall confine our attention to only cases where the variation is only along the azimuthal direction. We therefore ignore the radial coordinate in the rest of our discussion. The SoP of a vector beam will be represented as $|\mathbf{u}(\varphi)\rangle$ where φ is the azimuthal angle, measured from some reference axis, say the x axis. It can be represented as in Eq. (1):

$$|\mathbf{u}(\varphi)\rangle = u_l(\varphi)|\mathbf{l}\rangle + u_r(\varphi)|\mathbf{r}\rangle, \quad (31)$$

where $u_l(\varphi)$ and $u_r(\varphi)$ are complex periodic functions of the azimuthal angle φ : $u_l(2\pi + \varphi) = u_l(\varphi)$ and $u_r(2\pi + \varphi) = u_r(\varphi)$, and satisfying the normalization requirement $|u_l(\varphi)|^2 + |u_r(\varphi)|^2 = 1$. If the coefficients $u_l(\varphi)$ and $u_r(\varphi)$ depend identically on φ as $e^{im\varphi}$, for some integer m , we say the light beam carries an OAM of m units. We represent such states by the symbol $|\mathbf{u}; m\rangle$:

$$|\mathbf{u}; m\rangle \equiv |\mathbf{u}\rangle \otimes |m\rangle = |\mathbf{u}\rangle e^{im\varphi}, \quad (32)$$

where m is an integer and $|\mathbf{u}\rangle$ is a SoP of the form Eq. (1), having no azimuthal dependence. We refer to such light beams as scalar light beams. The SoPs along two different azimuthal angles on the transverse plane of such scalar light beams differ only in their global phase.

An arbitrary vector beam of the form Eq. (31) can be obtained as a superposition of a collection of such scalar beams, resulting in a composite state $|\mathbf{U}\rangle$ of the form Eq. (3). The Jones vector of its m^{th} OAM component and its amplitude can be extracted from $|\mathbf{u}(\varphi)\rangle$ as

$$u_m|\mathbf{u}_m\rangle = \int_0^{2\pi} e^{-im\varphi} |\mathbf{u}(\varphi)\rangle d\varphi \quad \forall m \in [b, e]. \quad (33)$$

The limits b and e in Eq. (33) are the smallest and largest m that yield nonzero u_m . We confine our attention to only those $\mathbf{u}(\varphi)$ for which the b and e are finite, i.e., only those vector beams which are constructed out of a superposition of a finite number of scalar beams having definite OAM. In such a case, there is a one-to-one correspondence between vector beams having a spatially SoP of the form Eq. (31) and composite quantum state of the form (3), $|\mathbf{u}(\varphi)\rangle \leftrightarrow |\mathbf{U}\rangle$, with Eq. (33) establishing the mapping. The corresponding orthogonal states also follow the same mapping $|\mathbf{u}(\varphi)_\perp\rangle \leftrightarrow |\mathbf{U}_\perp\rangle$, where $|\mathbf{u}(\varphi)_\perp\rangle$ is obtained through $|\mathbf{u}(\varphi)\rangle$ from Eq. (2), and $|\mathbf{U}_\perp\rangle$ is obtained through $|\mathbf{U}\rangle$ using Eq. (19).

A prominent method of generating such vector light beams has been using optical interferometers [67,68] with spatial light modulators [69–72]. They have also been generated by employing inhomogeneous wave plates called q plates [73] which are wave plates with uniform retardance, but whose orientation of the fast axis varies linearly with the azimuthal angle. We represent such q plates with the symbol $\hat{q}_\Gamma(q, \alpha_0)$, where Γ is called the retardance, q is called the topological charge, and α_0 is the offset-angle [74]. The import of these parameters can be understood by knowing its action on an arbitrary separable state $|\mathbf{u}; m\rangle$:

$$\hat{q}_\Gamma(q, \alpha_0)|\mathbf{u}; m\rangle = -\sin\frac{\Gamma}{2}\langle\mathbf{r}|\mathbf{u}\rangle e^{-2i\alpha_0}|\mathbf{l}; m-2q\rangle + \cos\frac{\Gamma}{2}|\mathbf{u}; m\rangle + \sin\frac{\Gamma}{2}\langle\mathbf{l}|\mathbf{u}\rangle e^{2i\alpha_0}|\mathbf{r}; m+2q\rangle. \quad (34)$$

A q plate of topological charge q and retardance π is called as the standard q plate. It raises the OAM of the left circular component of the input light beam by $2q$ units and simultaneously reduces the OAM of its right circular component by $2q$ units. The inverses of $\hat{p}_\Gamma(\alpha)$ and $\hat{q}_\Gamma(q, \alpha_0)$ are given by

$$\hat{p}_\Gamma(\alpha)^{-1} = \hat{p}_\Gamma\left(\alpha + \frac{\pi}{2}\right), \quad \hat{q}_\Gamma(q, \alpha_0)^{-1} = \hat{q}_\Gamma\left(q, \alpha_0 + \frac{\pi}{2}\right). \quad (35)$$

B. Coin based quantum walks on the SAM-OAM space

In the SAM-OAM implementation of quantum walks, the ‘‘coin-toss operation’’ is implemented using wave plates and the ‘‘shift operation’’ is implemented using q plates [45,46]. Since the initial state is normalized, and the involved q plates and wave plates are all unitary, an immediate constraint on

the emerging vector beams $|\mathbf{U}\rangle$ is that the corresponding SoP $|\mathbf{u}(\varphi)\rangle$ satisfies $\langle \mathbf{u}(\varphi) | \mathbf{u}(\varphi) \rangle = 1$ at all azimuthal angles φ . But this inner product can be evaluated as

$$\langle \mathbf{u}(\varphi) | \mathbf{u}(\varphi) \rangle = \sum_{m,n} u_m u_n \langle \mathbf{u}_m | \mathbf{u}_n \rangle e^{i(m-n)\varphi}. \quad (36)$$

The above double summation over m and n can be rewritten collecting terms having identical $m - n$ as

$$\langle \mathbf{u}(\varphi) | \mathbf{u}(\varphi) \rangle = \sum_{d=b-e}^{e-b} \left(\sum_{m=b}^{e-d} u_m u_{m+d} \langle \mathbf{u}_m | \mathbf{u}_{m+d} \rangle \right) e^{-id\varphi}, \quad (37)$$

where we take $u_m = 0$ for all $m < b$ or $m > e$. Pulling out the $d = 0$ term from the above summation, we have

$$\begin{aligned} \langle \mathbf{u}(\varphi) | \mathbf{u}(\varphi) \rangle &= \sum_{m=b}^e |u_m|^2 \\ &+ \sum_{d=b-e, d \neq 0}^{e-b} \left(\sum_{m=b}^{e-d} u_m u_{m+d} \langle \mathbf{u}_m | \mathbf{u}_{m+d} \rangle \right) e^{-id\varphi}. \end{aligned} \quad (38)$$

The first term of the left-hand side (LHS) of Eq. (38) is 1, since the u_m are components of the unit vector $|\mathbf{U}\rangle$ of the composite space. Therefore, for the inner product $\langle \mathbf{u}(\varphi) | \mathbf{u}(\varphi) \rangle$ to be equal to 1 at all φ , the second summation must vanish identically, at all φ . This is possible only when every term in its parenthesis is 0. This leads to the constraints which are exactly identical to those of Eq. (16), and their complex conjugates. Therefore, this forces us to conclude that a composite state $|\mathbf{U}\rangle$ of the form Eq. (3) is a walk state in the SAM-OAM space of the light beams, only if the corresponding SoP is normalized at every azimuthal angle φ : that is, $\langle \mathbf{u}(\varphi) | \mathbf{u}(\varphi) \rangle = 1 \forall \varphi$. In the rest of this section, we focus our attention to such vector beams only.

The aim now is to generate such vector beams using only wave plates and q plates. With respect to DTQWs, the standard q plates mimic the standard shift operator, Eq. (6), except that here apart from altering the OAM of the light, the standard q plate also swaps the circular polarization components. A q plate with $\Gamma \neq \pi$ functions like a standard q plate but only on a fraction $\sin \frac{\Gamma}{2}$ of the incident light beam. Currently, q plates whose retardance Γ can be tuned by varying the applied voltage have been designed [75,76] and are also commercially available [77]. Likewise, the so-called Berek plate functions like a homogeneous wave plate but with a tunable retardance [78]. In this context, the effective behavior of a collection of three wave plates and q plates has been explored in Refs. [79] and [74]. To make connection between the q plate and the quantum step of Eq. (11), we have the following relation: $\hat{q}_\Gamma(q, \alpha_0) = \hat{T}_\Gamma(2\alpha_0, 2q, \mathbf{I}, \mathbf{I})$. It is possible to implement the quantum step \hat{T}_π , that is T_Γ of Eq. (11) with $\Gamma = \pi$, using a pair of wave plates and a single q plate:

$$\hat{T}_\pi(\delta, p, s, c) \equiv \hat{p}_{r_2}(\alpha_2) \hat{q}_\pi\left(\frac{p}{2}, \alpha_0\right) \hat{p}_{r_1}(\alpha_1), \quad (39)$$

where the parameters of the plate are given as

$$\begin{aligned} \Gamma_1 &= 2 \tan^{-1} \left(\frac{|(\mathbf{r}|\mathbf{c})|}{|(\mathbf{l}|\mathbf{c})|} \right), \\ \alpha_1 &= \frac{\pi}{2} + \frac{1}{2} [\Phi((\mathbf{r}|\mathbf{c})) - \Phi((\mathbf{l}|\mathbf{c}))], \\ \alpha_0 &= \frac{1}{2} [\delta - \Phi((\mathbf{l}|\mathbf{c})) - \Phi((\mathbf{l}|\mathbf{s}))], \\ \Gamma_2 &= 2 \tan^{-1} \left(\frac{|(\mathbf{r}|\mathbf{s})|}{|(\mathbf{l}|\mathbf{s})|} \right), \\ \alpha_2 &= \frac{1}{2} [\Phi((\mathbf{r}|\mathbf{s})) - \Phi((\mathbf{l}|\mathbf{s}))]. \end{aligned} \quad (40)$$

The three-plate gadget involving a q_π plate introduced through Eqs. (39) and (40) can reproduce any \hat{T}_π quantum step. Replacing the q_π plate with a q_Γ plate, it can even reproduce any \hat{T}_Γ quantum step of Eq. (11), but only if $\Phi((\mathbf{l}|\mathbf{c})) = \Phi((\mathbf{l}|\mathbf{s}))$. This may appear as an obstacle in our attempt to obtain desired vector beams by means of quantum walks. However, recall that the shrinking algorithm places no restriction on the shift state $|\mathbf{s}\rangle$. We can exploit this freedom on $|\mathbf{s}\rangle$, not only to overcome the restriction on phase, but also to get rid of one of the plates altogether. The choice of $|\mathbf{s}\rangle = e^{i\Phi((\mathbf{l}|\mathbf{c}))} |\mathbf{l}\rangle$ satisfies the phase relation and also ensures that $\Gamma_2 = 0$, so that the second homogeneous wave plate need not be used at all, and one can work with only a pair of homogeneous wave plate and $q = \frac{1}{2} q$ plate per step.

VII. ILLUSTRATIONS

In this section, we shall provide some concrete examples for the concepts and notions introduced in the previous sections of this paper. Towards this, in Sec. VII A we propose a graphical notation for representing composite states and quantum walks. Using this graphical notation, we present a few illustrations of the shrinking algorithm and steered quantum walks in Sec. VII B. In Sec. VII C we provide illustrations implementing these two algorithms in the SAM-OAM space of light beams.

A. A novel representation for the qubit-qudit space

1. Representing composite states

Normalized qubit states of the form (1) can be elegantly described on the surface of a unit sphere called the Bloch sphere (which in the polarization setting is termed as the Poincaré sphere [78]). This treatment, in addition to providing a visualization of quantum states, also aids in giving a geometric picture of the action of SU(2) operators on such quantum states. In the polarization setting, the notion of Poincaré sphere has been extended to represent the composite states like Eq. (3), but limited to only two terms [80,81].

In this paper, we introduce a new graphical way of indicating coin states $|\mathbf{c}\rangle$ of the form Eq. (1). In this representation, the following holds:

(i) States of the form $\frac{1}{\sqrt{2}}(e^{i\theta_0} |\mathbf{0}\rangle + e^{i\theta_1} |\mathbf{1}\rangle)$ are depicted as a single purple-colored circle, of radius proportional to $\frac{1}{\sqrt{2}}$, with yellow and cyan colored arrows making angles θ_0 and θ_1 with the x axis, respectively.

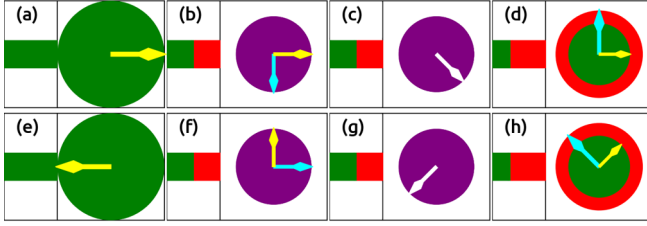


FIG. 1. The top row [panels (a)–(d)] depicts the four coin states $|\mathbf{0}\rangle$, $|\mathbf{h}\rangle \equiv \frac{1}{\sqrt{2}}(|\mathbf{0}\rangle - i|\mathbf{1}\rangle)$, $|\mathbf{d}\rangle \equiv \frac{e^{-i\pi/4}}{\sqrt{2}}(|\mathbf{1}\rangle + |\mathbf{0}\rangle)$, and $|\mathbf{u}\rangle \equiv \frac{1}{\sqrt{3}}(|\mathbf{0}\rangle + i\sqrt{2}|\mathbf{1}\rangle)$, and the bottom row [panels (e)–(h)] depict the states $-\mathbf{0}\rangle$, $i|\mathbf{h}\rangle$, $-i|\mathbf{d}\rangle$, and $e^{i\pi/4}|\mathbf{u}\rangle$. The purple circles correspond to the states where the $|\mathbf{0}\rangle$ and $|\mathbf{1}\rangle$ components are of the same magnitude. In other cases, the green circle corresponds to the $|\mathbf{0}\rangle$ component, its radius proportional to the magnitude of that component and its phase is indicated by a yellow arrow. The red circle corresponds to the $|\mathbf{1}\rangle$ component, its radius being proportional to the magnitude of that component and its phase is indicated by a cyan arrow. At each position, green and red rectangles are also drawn, whose widths are proportional to the intensity in the $|\mathbf{0}\rangle$ and $|\mathbf{1}\rangle$ components at that position, respectively.

(ii) States of the form $\frac{e^{i\theta}}{\sqrt{2}}(|\mathbf{0}\rangle + |\mathbf{1}\rangle)$ are depicted with a purple-colored circle of radius proportional to $\frac{1}{\sqrt{2}}$, and a single white-colored arrow making an angle θ with the x axis.

(iii) Rest of the states $|\mathbf{c}\rangle$, we indicate in terms of the two complex numbers, c_0 and c_1 , the components of $|\mathbf{c}\rangle$ along $|\mathbf{0}\rangle$ and $|\mathbf{1}\rangle$ unit vectors, respectively. We represent these complex numbers as two concentric green and red circles of radii proportional to $|c_0|$ and $|c_1|$, respectively. The phase of these complex numbers are indicated by yellow and cyan colored arrows over these circles, the angles they make with the horizontal indicative of their phases.

Bloch sphere or polarization ellipse representations represent a state only up to a global phase. They are therefore not capable of depicting uniquely two coin states which differ only in their global phase. In the current representation, on the other hand, it is possible to represent a state completely, including its global phase. Figure 1, for example, shows eight coin states illustrated in our graphical notation. These are depicted in two rows. The bottom four states differ from the corresponding states in the top only in the global phase. It is evident that this notation assigns distinct representations to coin states that differ only in their global phase. The relative phase can also be easily read from the graphical representation: it is the angle that the cyan arrow makes with the yellow arrow, measured in the clockwise direction. Coin states with zero relative phase are represented by a single white arrow.

Another advantage of this graphical representation is that the graphical representation of the $|\mathbf{c}_\perp\rangle$ can be built from that of $|\mathbf{c}\rangle$ as (i) the green and red circles of $|\mathbf{c}_\perp\rangle$ will be the red and circles of $|\mathbf{c}\rangle$, respectively, (ii) the yellow arrow of $|\mathbf{c}_\perp\rangle$ will be the cyan arrow of $|\mathbf{c}\rangle$ reflected with respect to the y axis, and (iii) the cyan arrow of $|\mathbf{c}_\perp\rangle$ will be the yellow arrow of $|\mathbf{c}\rangle$ reflected with respect to the x axis. An orthogonal pair of coin states can therefore be easily identified from their graphical representation. The graphical construction of orthogonal states also respects the relation $|\mathbf{u}_\perp\rangle = -|\mathbf{u}\rangle$, as expected. For illustration, the orthogonal states for each of the eight states of Fig. 1 are depicted in Fig. 2.

This representation can be used to depict composite states as well. We depict the composite state $|\mathbf{P}\rangle$ of Eq. (3) as follows: on the y axis we mark the walk space basis states $|m\rangle$ from $m \in [b, e]$. At every m with nonzero p_m , the corresponding coin state $|\mathbf{p}_m\rangle$ is depicted as described above, except that the radii of these circles is scaled by the amplitude p_m . For illustration of the graphical notation, consider the following six composite states of the form (3):

$$\begin{aligned}
 |\mathbf{A}\rangle &= \frac{1}{\sqrt{2}}(|\mathbf{a}, -1\rangle + |\mathbf{d}, 2\rangle), \\
 |\mathbf{B}\rangle &= \frac{1}{\sqrt{3}}(|\mathbf{h}, 0\rangle - |\mathbf{a}, 1\rangle + |\mathbf{v}, 2\rangle), \\
 |\mathbf{C}\rangle &= \frac{1}{2}(|\mathbf{h}, -2\rangle - \sqrt{2}|\mathbf{a}, 0\rangle + |\mathbf{v}, 2\rangle), \\
 |\mathbf{D}\rangle &= \frac{1}{\sqrt{5}}(|\mathbf{d}, -2\rangle + |\mathbf{l}, -1\rangle - |\mathbf{r}, 0\rangle + i|\mathbf{l}, 1\rangle + i|\mathbf{a}, 2\rangle), \\
 |\mathbf{E}\rangle &= \frac{1}{2}(|\mathbf{c}, -2\rangle - \sqrt{2}|\mathbf{h}, -1\rangle + |\mathbf{e}, 1\rangle), \\
 |\mathbf{F}\rangle &= \frac{1}{\sqrt{5}}(i|\mathbf{c}, -2\rangle + |\mathbf{l}, -1\rangle + |\mathbf{e}, 0\rangle + |\mathbf{r}, 1\rangle + |\mathbf{c}, 2\rangle),
 \end{aligned} \tag{41}$$

where $|\mathbf{h}\rangle$, $|\mathbf{v}\rangle$ are a pair of orthogonal states $|\mathbf{h}\rangle = \frac{1}{\sqrt{2}}(|\mathbf{0}\rangle - i|\mathbf{1}\rangle)$, and $|\mathbf{v}\rangle = \frac{1}{\sqrt{2}}(|\mathbf{1}\rangle - i|\mathbf{0}\rangle)$, and states $|\mathbf{d}\rangle$, $|\mathbf{a}\rangle$ are another pair of orthogonal states: $|\mathbf{d}\rangle = \frac{e^{-i\pi/4}}{\sqrt{2}}(|\mathbf{1}\rangle + |\mathbf{0}\rangle)$, and $|\mathbf{a}\rangle = \frac{e^{i\pi/4}}{\sqrt{2}}(|\mathbf{1}\rangle - |\mathbf{0}\rangle)$, and $|\mathbf{c}\rangle$ and $|\mathbf{e}\rangle$ are yet another orthogonal pair $|\mathbf{c}\rangle = \frac{1}{2}(\sqrt{3}|\mathbf{0}\rangle + i|\mathbf{1}\rangle)$ and $|\mathbf{e}\rangle = \frac{1}{2}(i|\mathbf{0}\rangle + \sqrt{3}|\mathbf{1}\rangle)$, all belonging to the coin space. All the six states are normalized. Of these, the first state has the position span of $[-1, 2]$, the second state, $|\mathbf{B}\rangle$ has the position span $[0, 2]$, $|\mathbf{E}\rangle$ has the position span of $[-2, 1]$, and the rest of the states have the position span $[-2, 2]$.

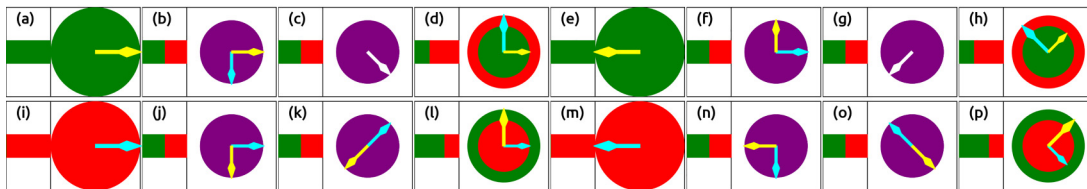


FIG. 2. Graphical illustration of the orthogonal pair of states. The top row depicts the eight states of Fig. 1, and the bottom row depicts their orthogonal states.

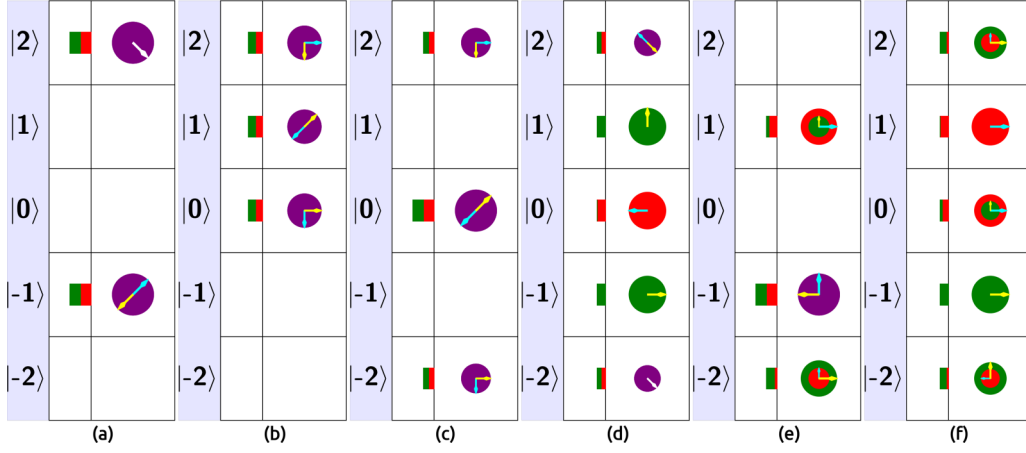


FIG. 3. The six composite states of Eq. (41) depicted in our graphical notation. Each of these composite states $|\mathbf{P}\rangle$ are represented in terms of their coin states $|\mathbf{p}_m\rangle$ for m being $[-2, \dots, 2]$. The representation of the coin states is the same as discussed in Fig. 1, except that the radii of the circles are now scaled by the amplitude p_m of that component.

Figure 3 depicts these six composite states of Eq. (41) in the new graphical notation.

Given the graphical representation of a composite state $|\mathbf{U}\rangle$, the graphical representation of its orthogonal state $|\mathbf{U}_\perp\rangle$ can be easily constructed, since the coin states of $|\mathbf{U}_\perp\rangle$ are orthogonal states of the coin states of $|\mathbf{U}\rangle$ [see Eq. (19)]. To show this relationship between the orthogonal composite states, in Fig. 4 we plot the pairs of orthogonal states $|\mathbf{A}\rangle$, $|\mathbf{A}_\perp\rangle$, $|\mathbf{B}\rangle$, $|\mathbf{B}_\perp\rangle$, $|\mathbf{I}\rangle$, $|\mathbf{I}_\perp\rangle$ and $|\mathbf{J}\rangle$, $|\mathbf{J}_\perp\rangle$ where $|\mathbf{A}\rangle$ and $|\mathbf{B}\rangle$ given in (41), and the states $|\mathbf{I}\rangle = \frac{1}{\sqrt{2}}(|\mathbf{0}\rangle, 1) + \sqrt{3}|\mathbf{1}\rangle, 2)$ and $|\mathbf{J}\rangle = \frac{1}{\sqrt{3}}(|\mathbf{u}, 0) + \sqrt{2}|\mathbf{w}, 2)$. Here $|\mathbf{u}\rangle = \frac{1}{\sqrt{3}}(|\mathbf{0}\rangle + i\sqrt{2}|\mathbf{1}\rangle)$, and $|\mathbf{w}\rangle = \frac{1}{2}(|\mathbf{0}\rangle + i\sqrt{3}|\mathbf{1}\rangle)$.

2. Representing quantum steps and quantum walks

The quantum steps can also be represented in the graphical notation using the same representation as that of the composite states. We depict quantum steps $\hat{T}_\Gamma(\delta, p, s, \mathbf{c})$ in terms of their action on the orthogonal pair of home states $|\mathbf{c}; 0\rangle$ and $|\mathbf{c}_\perp; 0\rangle$. The two input home states $|\mathbf{c}; 0\rangle$ and $|\mathbf{c}_\perp; 0\rangle$,

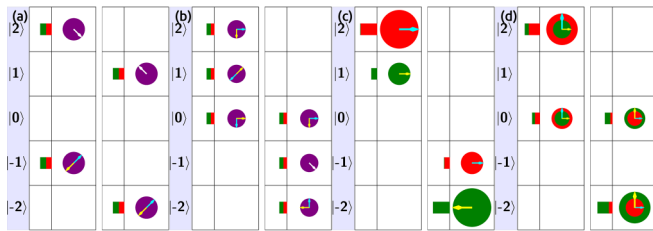


FIG. 4. Depicting the orthogonal composite states in the current graphical representation. Four states and their orthogonal states are depicted. The subfigure (a) depicts the pair of states $|\mathbf{A}\rangle$ and $|\mathbf{A}_\perp\rangle$, subfigure (b) depicts the pair $|\mathbf{B}\rangle$ and $|\mathbf{B}_\perp\rangle$, subfigure (c) depicts the pair $|\mathbf{I}\rangle$ and $|\mathbf{I}_\perp\rangle$, and subfigure (d) depicts the pair $|\mathbf{J}\rangle$ and $|\mathbf{J}_\perp\rangle$. The states $|\mathbf{A}\rangle$ and $|\mathbf{B}\rangle$ are defined in Eq. (41), and the composite states $|\mathbf{I}\rangle$ and $|\mathbf{J}\rangle$ are $|\mathbf{I}\rangle = \frac{1}{\sqrt{2}}(|\mathbf{0}\rangle, 1) + \sqrt{3}|\mathbf{1}\rangle, 2)$ and $|\mathbf{J}\rangle = \frac{1}{\sqrt{3}}(|\mathbf{u}, 0) + \sqrt{2}|\mathbf{w}, 2)$. Here $|\mathbf{u}\rangle = \frac{1}{\sqrt{3}}(|\mathbf{0}\rangle + i\sqrt{2}|\mathbf{1}\rangle)$, and $|\mathbf{w}\rangle = \frac{1}{2}(|\mathbf{0}\rangle + i\sqrt{3}|\mathbf{1}\rangle)$.

and the two output composite states $\hat{T}_\Gamma(\delta, p, s, \mathbf{c})|\mathbf{c}; 0\rangle$ and $\hat{T}_\Gamma(\delta, p, s, \mathbf{c})|\mathbf{c}_\perp; 0\rangle$ are all depicted in the concentric circle representation of states introduced earlier. A quantum walk \hat{W} of the form Eq. (13) is represented with such steps stacked from the right to left, with the first step appearing rightmost and the last step appearing leftmost. As an illustration of a quantum walk, a seven steps walk is depicted in Fig. 5. The first and six steps of this walk are improper steps, the fifth step is of size $d = 2$, and rest of the steps are of unit size.

B. Examples of quantum walks

1. Identifying walk and non-walk states

As first illustrations of walk and non-walk states, consider the product states in the composite space. They are of the form $|\mathbf{u}\rangle \otimes |\mathbf{s}\rangle$, where $|\mathbf{u}\rangle \in \text{span}(|\mathbf{0}\rangle, |\mathbf{1}\rangle)$ and $|\mathbf{s}\rangle \in \text{span}(\dots, |-\mathbf{1}\rangle, |\mathbf{0}\rangle, |\mathbf{1}\rangle, \dots)$. Of these, the only possible translation invariant product states are of the form $|\mathbf{u}; m\rangle$, where $|m\rangle \in (\dots, |-\mathbf{1}\rangle, |\mathbf{0}\rangle, |\mathbf{1}\rangle, \dots)$. A composite state with only two nonzero OAM components, $|\mathbf{W}\rangle = w_b|\mathbf{w}_b; b) + w_e|\mathbf{w}_e; e)$ is a walk state only if the two constituent coin states are orthogonal: $\langle \mathbf{w}_b | \mathbf{w}_e \rangle = 0$. The state $|\mathbf{A}\rangle$ defined in Eq. (41) is of this form and therefore it is a walk state. Similarly, a composite state $|\mathbf{X}\rangle$ consisting of three constituent terms: $|\mathbf{X}\rangle = x_b|\mathbf{x}_b; b) + x_m|\mathbf{x}_m; m) + x_e|\mathbf{x}_e; e)$ where b, m , and e are integers and x_b, x_m , and x_e are real numbers such that $x_b^2 + x_m^2 + x_e^2 = 1$, is a walk state only if

$$m = \frac{b + e}{2},$$

$$|\mathbf{x}_m\rangle = \frac{1}{\sqrt{x_e^2 + x_b^2}}(e^{i\delta}x_e|\mathbf{x}_b\rangle - e^{-i\delta}x_b|\mathbf{x}_e\rangle),$$

$$\langle \mathbf{x}_b | \mathbf{x}_e \rangle = 0,$$

where δ is an arbitrary phase. This is an interesting result, with respect to the state engineering aspect of the quantum walks. The first of these restricts the possible occupied positions of a three-term walk state. It is not possible via quantum walks to access composite states where, for instance, only the $|\mathbf{0}\rangle$,

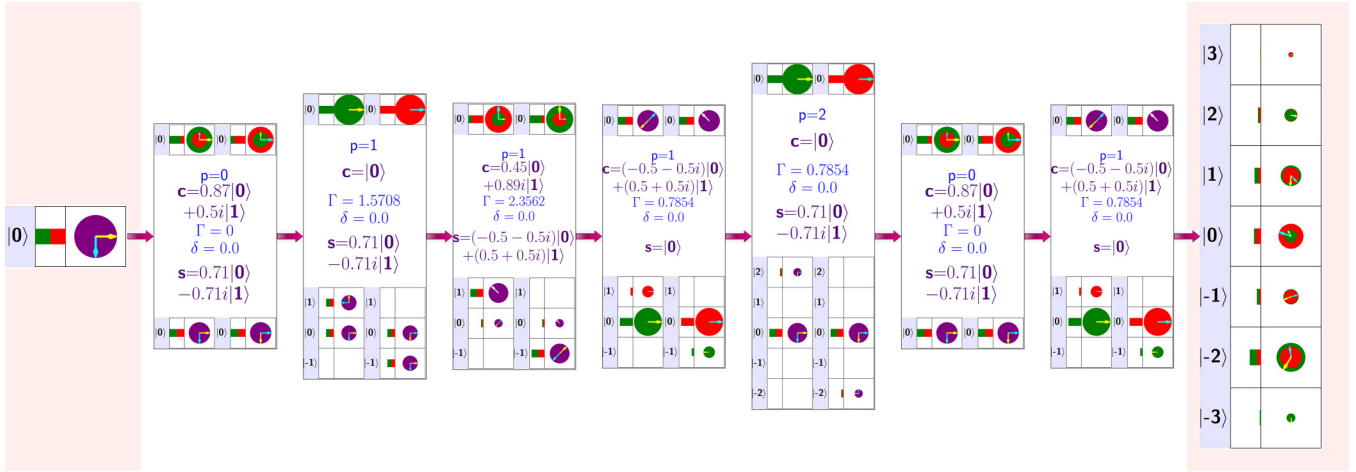


FIG. 5. A quantum walk of seven steps, starting from the home state $|h; 0\rangle$. At the end of the seventh step, the resulting composite state is the one spanning the positions $[-3, 3]$, with probabilities P_m being $[0.021, 0.355, 0.117, 0.214, 0.197, 0.089, 0.007]$ for $m = -3, \dots, 3$.

$|1\rangle$, and $|3\rangle$ position states are occupied. And this is true irrespective of the corresponding amplitudes of occupation x_0 , x_1 , and x_2 and the coin states $|x_0\rangle$, $|x_1\rangle$, and $|x_3\rangle$. From this it can also be seen that the states $|B\rangle$ and $|C\rangle$ defined in Eq. (41) are walk states, but the state $|E\rangle$ of Eq. (41) is not.

Consider now the four-component state

$$|Y\rangle = y_b|y_b; b\rangle + y_m|y_m; m\rangle + y_n|y_n; n\rangle + y_e|y_e; e\rangle,$$

where b , m , n , and e are integers and y_b , y_m , y_n , and y_e are nonzero real numbers such that $y_b^2 + y_m^2 + y_n^2 + y_e^2 = 1$. It follows from Eq. (16) that $|Y\rangle$ is a walk state, if and only if $m - b = e - n$. Furthermore, if $e - b \neq m - n (= e - n)$, then it is a walk state only if the amplitudes satisfy the relation $y_b/y_m = y_e/y_n$, and the coin states satisfy the relations $\langle y_b|y_m\rangle = \langle y_n|y_e\rangle = 0$ and $\langle y_b|y_n\rangle + \langle y_m|y_e\rangle = 0$.

Of the six states defined in Eq. (41), and depicted in Fig. 3, it can be seen that only the first four states are walk states satisfying the constraints Eq. (16).

2. Constructing new walks from existing ones

We now provide a couple of illustrations for constructing new walk states of larger span from linear combination of walk states with smaller span, the basic idea of which was introduced earlier in Sec. III C. Consider the five-component state $|D\rangle$ of Eq. (41). Its position span is $[-2, 2]$. The position span of $|D_{+3}\rangle$ is therefore $[1, 5]$. Its orthogonal state $|(\mathbf{D}_{+3})_\perp\rangle$ therefore has a span of $[-5, -1]$. A complex combination of these two states $\alpha|D_{+3}\rangle + \beta|(\mathbf{D}_{+3})_\perp\rangle$ where $|\alpha|^2 + |\beta|^2 = 1$ will be walk states with position span $[-5, 5]$. One such walk state is

$$\begin{aligned} |G\rangle &= \frac{1}{\sqrt{2}}(|D_{+3}\rangle + |(\mathbf{D}_{+3})_\perp\rangle) \\ &= \frac{1}{\sqrt{10}}(i|d; -5\rangle - i|r; -4\rangle + |l; -3\rangle + |r; -2\rangle + |a; -1\rangle \\ &\quad + |d; 1\rangle + |l; 2\rangle - |r; 3\rangle + i|l; 4\rangle + i|a; 5\rangle). \end{aligned} \quad (42)$$

State $|G\rangle$ has the position span of $[-5, 5]$, in which for all nonzero $m \in [-5, 5]$, the probability P_m is $1/10$. One could

likewise generate a ten-term “uniform walk state” from $|D\rangle$ as

$$\begin{aligned} |H\rangle &= \frac{1}{\sqrt{2}}[|D_{\times 2}\rangle + |((\mathbf{D}_{\times 2})_\perp)_{+1}\rangle] \\ &= \frac{1}{\sqrt{10}}(|d; -4\rangle + i|d; -3\rangle + |l; -2\rangle - i|r; -1\rangle - |r; 0\rangle \\ &\quad + |l; 1\rangle + i|l; 2\rangle + |r; 3\rangle + i|a; 4\rangle + |a; 5\rangle), \end{aligned} \quad (43)$$

where $|D_{\times 2}\rangle$ is the state that is obtained from $|D\rangle$ by Eq. (17), state $|(\mathbf{D}_{\times 2})_\perp\rangle$ is its orthogonal state, and the state $|((\mathbf{D}_{\times 2})_\perp)_{+1}\rangle$ is $|(\mathbf{D}_{\times 2})_\perp\rangle$ translated by one unit. State $|H\rangle$ has the position span of $[-4, 5]$, in which for all $m \in [-4, 5]$, including $m = 0$, the occupation probability P_m is $1/10$.

3. Illustrations of the steered quantum-walk algorithm

As illustrations of the steered quantum-walk algorithm discussed in Sec. IV, we show the evolution of home states into each of the four walk states of Eq. (41). As $N = \max(|b|, |e|)$ is equal to 2 for all four states, they can be generated in just two proper steps. The required steps, the initial home states and the intermediate walk states are all depicted in Fig. 6. While the states $|A\rangle$ and $|B\rangle$ are generated with $|l; 0\rangle$ as the home state, the other two are generated with home states $e^{i\frac{3\pi}{4}}|a; 0\rangle$ and $|d; 0\rangle$, respectively. In each of the four quantum walks, the coin states $|c\rangle$ of both the steps are taken be $|0\rangle$.

4. Simplification of quantum walks

For an illustration of the simplification of a quantum walk \hat{W} discussed in Sec. V A, consider the seven-step quantum walk depicted in Fig. 5. Recall that of the seven steps there, two were improper; that is, pure $SU(2)$ transformations in the coin space, one step was of $d = 2$, and remaining four steps were of $d = 1$. But since the position span of the resulting composite state is $[-3, 3]$, this state can also be obtained from the home state in just three $d = 1$ steps, using our steered quantum walk algorithm. This three-step minimal walk is depicted in Fig. 7.

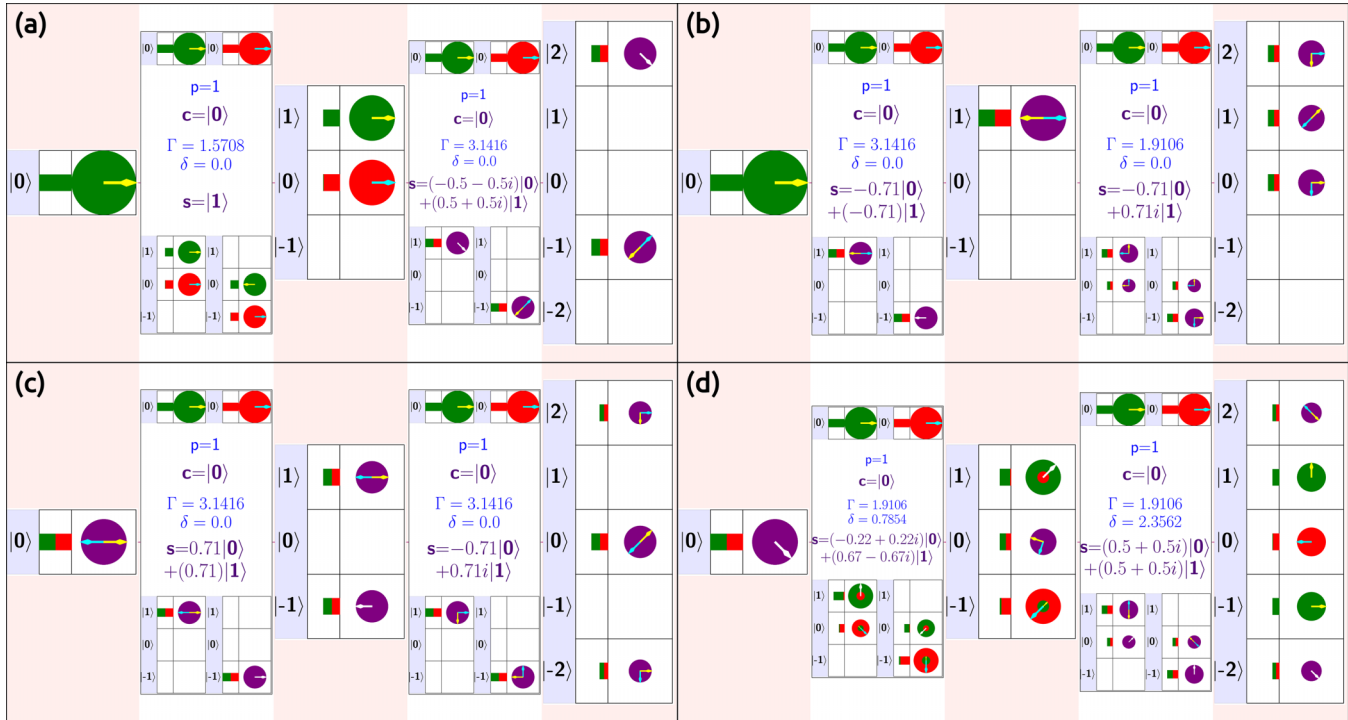


FIG. 6. Targeted quantum walks to generate each of the four walk states of Eq. (41) starting from home states, in two steps of unit step size. Panels (a)–(d) correspond to the states $|A\rangle$, $|B\rangle$, $|C\rangle$, and $|D\rangle$, respectively.

5. Transformation between walk states

As an illustration of transforming one walk state to another as detailed in Sec. VB, consider the transformation of the state $|D\rangle$ of Eq. (41), to the walk state $i|D\rangle$. The two states differ only by an overall phase factor but the quantum walk that accomplishes the transformation is far from trivial. This

is accomplished by a four-step quantum walk. The four-step minimal quantum walk obtained by the minimization procedure elaborated above is shown in Fig. 8. From this graphical representation it is clear that the quantum walk actually proceeds in two phases: in the first phase consisting of two steps, the state $|D\rangle$ is taken to the home state $\frac{1}{\sqrt{2}}(|0\rangle + i|1\rangle)$, and in

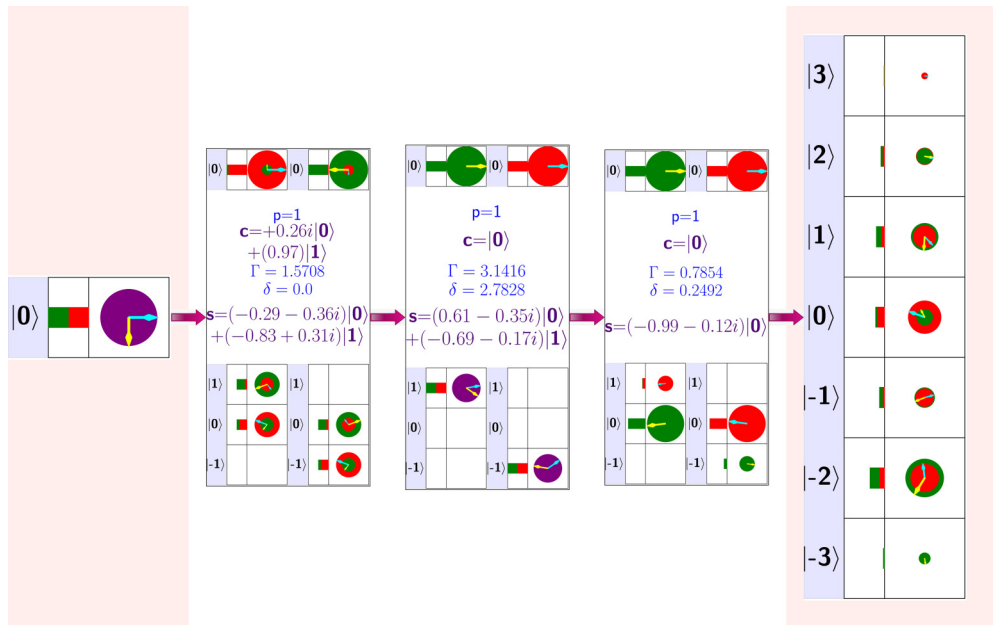


FIG. 7. The three-step quantum walk that is equivalent to the seven-step quantum walk depicted in Fig. 5. Note that the initial and final are the same as those in Fig. 5.

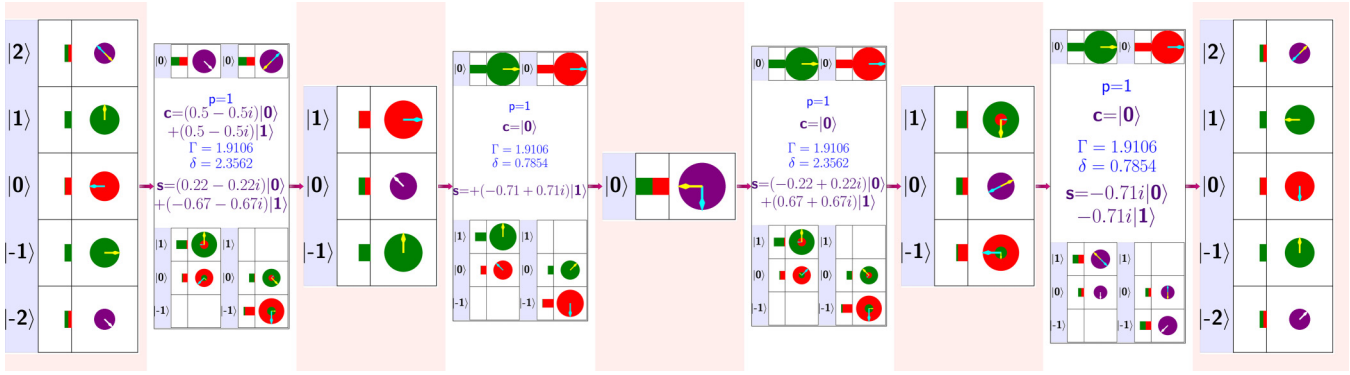


FIG. 8. A minimal quantum walk for transforming the state $|D\rangle$ of Eq. (41) to the state $i|D\rangle$. The walk is four steps long.

the second phase consisting of the next two steps, the home state $\frac{1}{\sqrt{2}}(|0\rangle + i|1\rangle)$ is taken to the target state $i|D\rangle$.

C. SAM-OAM implementation of quantum walks

1. Walk states on the SAM-OAM space

Recall the result derived earlier that a composite state $|U\rangle$ is realizable using q plates and wave plates provided the corresponding SoP $|\mathbf{u}(\varphi)\rangle$ has a norm equal to 1 at all φ . In this section, we examine this result in the context of the six composite states defined in Eq. (41), and also the two states $|G\rangle$ and $|H\rangle$ defined in Eqs. (42) and (43). Towards this, for each of these states, we compute the sum of the intensities in the right- and left-circular components, as a function of azimuthal angle, as shown in Fig. 9. This figure comprises of eight subfigures, and in each of them, we have plotted the polar plot of the right circular component $|\langle r|\mathbf{u}(\varphi)\rangle|^2$ in red, the left-circular component $|\langle l|\mathbf{u}(\varphi)\rangle|^2$ in green, and their sum in blue, with $\mathbf{u}(\varphi)$ being the equivalent SoP of the composite state $|U\rangle$, with $|U\rangle$ being one of the eight states $|A\rangle, \dots, |H\rangle$,

respectively. It is evident that in case of the six walk states, the sum of the field intensity components, i.e., the blue plot, remains at 1 at all azimuthal angles, whereas in case of the non-walk states $|E\rangle$ and $|F\rangle$, the total field intensity varies with the azimuthal angle, exceeding 1 at some azimuth and succeeding 1 at some azimuths.

2. Graphical notation of vector beams

A standard method for representing SoPs has been as polarization ellipses [82]. In this notation, the SoPs are depicted as ellipses, with ellipticity e and orientation ϕ given by

$$e = \frac{|\langle l|\mathbf{u}\rangle|^2 - |\langle r|\mathbf{u}\rangle|^2}{|\langle l|\mathbf{u}\rangle|^2 + |\langle r|\mathbf{u}\rangle|^2},$$

$$\phi = \Phi(\langle r|\mathbf{u}\rangle) - \Phi(\langle l|\mathbf{u}\rangle) + \frac{\pi}{4}. \quad (44)$$

These definitions are not standard, but have been employed here due to their simplicity. Furthermore, since the ellipticity e is defined as the absolute value of the difference between the right and left circular intensities, this representation cannot distinguish the two states differing only in their helicity, a

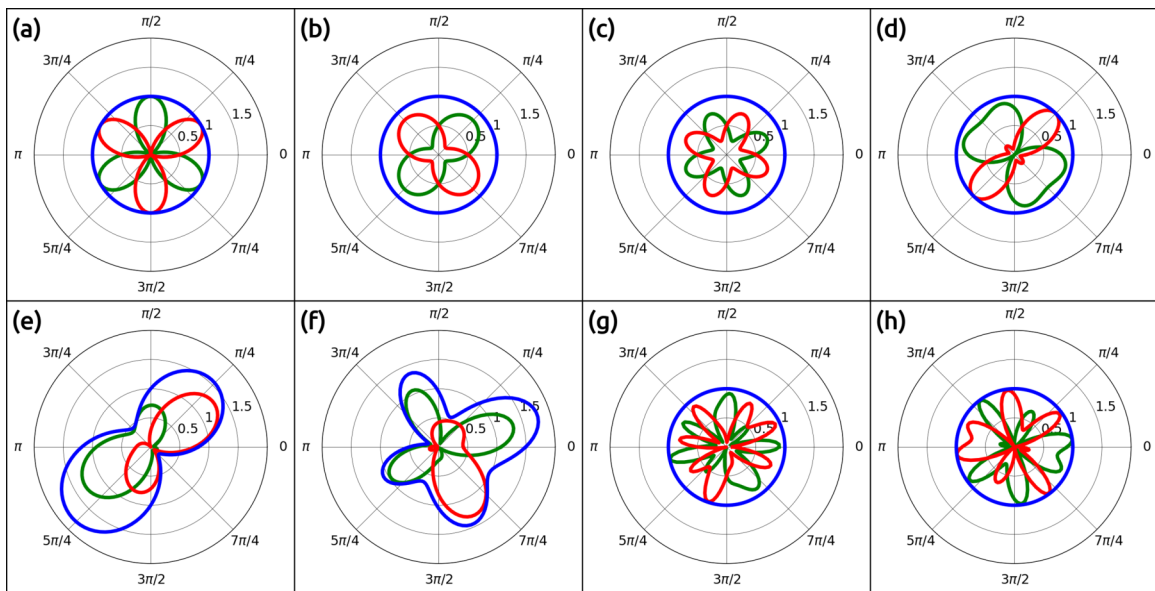


FIG. 9. Polar plot the intensity distribution of the six composite states of Eq. (41), state $|G\rangle$ of Eq. (42) and $|H\rangle$ of Eq. (43), as a function of the azimuthal angle. The green and red plots correspond to the intensity in the left and right circular polarization components, while the blue plot corresponds to the total, that is the sum of these intensities.

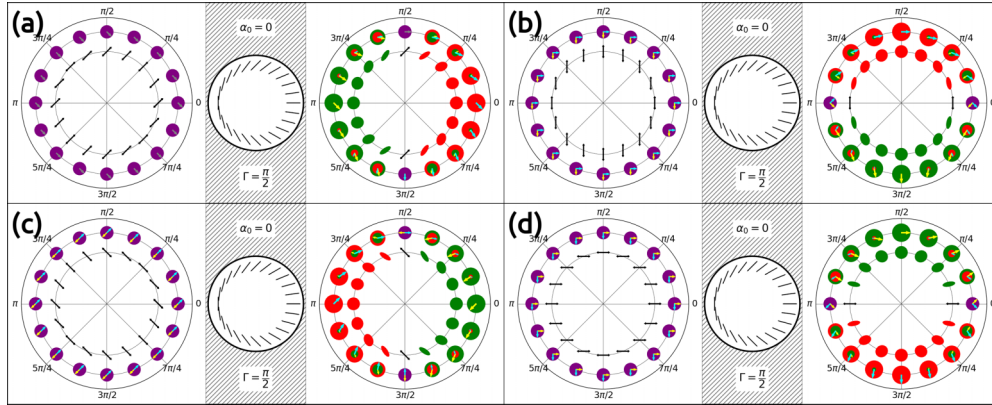


FIG. 10. (a)–(d) Action of a $q = \frac{1}{2} q$ plate with $\Gamma = \frac{\pi}{2}$ and $\alpha_0 = 0$, on four linearly polarized light beams, $|d\rangle$, $|v\rangle$, $|a\rangle$, and $|h\rangle$, respectively, having zero OAM. The input and output beams are represented in terms of the concentric-circle notation introduced earlier and also in the standard notation of the polarization ellipses. The orientation of short lines inside the q plates indicate the fast-axis orientation at that azimuthal angle.

well-known limitation of this method. To overcome this limitation, we color-code the ellipse to indicate the helicity: states with $|\langle l|u\rangle| > |\langle r|u\rangle|$ are colored green, those with $|\langle l|u\rangle| < |\langle r|u\rangle|$ are colored red, and those with $|\langle l|u\rangle| = |\langle r|u\rangle|$ are colored purple. Recall that the polarization ellipses representation depicts a SoP only up to a phase.

In this paper, the azimuthally varying SoP of the vector beams is depicted in both the methods: (i) as polarization ellipses and (ii) as the concentric circles of the graphical notation. To map the two representations: the circular polarizations are represented by green and red circles in both the representations. Purple circles in the concentric-circle representation corresponds to purple arrows in the elliptical representation.

3. Illustration of targeted quantum walks

We now provide some illustration of the shrinking algorithm and the steered quantum walk as implemented using q -plates and wave plates. But before doing that, we give a quick recall of the action of q plates on scalar light beams. This will also help in connecting our new notation of representing the SoPs with the standard polarization ellipses representation.

Figures 10 and 11 depict the action of $\Gamma = \frac{\pi}{2}$ and $\Gamma = \pi$ q -plates on four linearly polarized scalar light beams. In both the cases, the emergent light beam is a vector beam. While the vector beams emerging in the former case are identical fraction of left and right helicity components, in the latter case the vector beam is composed only of plane-polarized SoPs.

We first provide an illustration of the shrinking algorithm for transforming the states $|G\rangle$ and $|H\rangle$ of Eqs. (42) and (43) into standard scalar light beams. Recall that $N = \max(|b|, |e|)$ of both the states is five, hence they both can be reduced in five quantum steps; that is, five pair of wave plates and q plates. Figure 12 shows the transverse plane polarization profiles of both the beams, as they progress through each pair of plates. We now look to generate the vector beams corresponding to the four walk states $|A\rangle, \dots, |D\rangle$ of Eq. (41). Since $N = 2$ for all the four states, each of them can be generated from standard scalar light beams by using just two pairs of wave plates and q plates. This conversion is demonstrated in Fig. 13. This is the SAM-OAM implementation of the quantum walk depicted in Fig. 6.

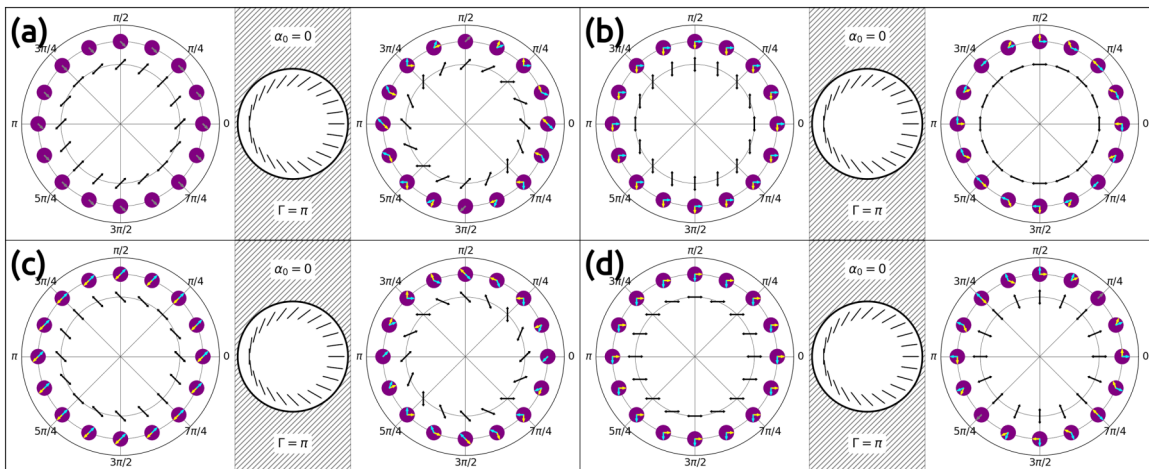


FIG. 11. (a)–(d) Action of a $q = \frac{1}{2} q$ plate with $\Gamma = \pi$ and $\alpha_0 = 0$, on four linearly polarized light beams, $|d\rangle$, $|v\rangle$, $|a\rangle$, and $|h\rangle$, respectively, having zero OAM. The orientation of short lines inside the q plates indicate the fast-axis orientation at that azimuthal angle.

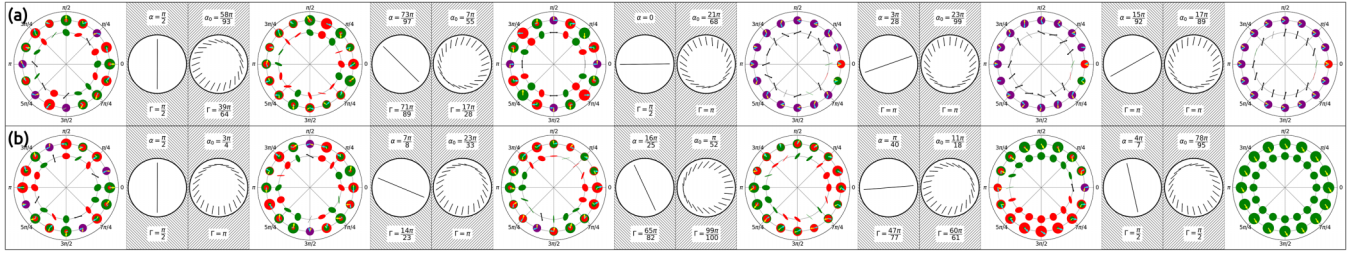


FIG. 12. Conversion of the vector beams $|G\rangle$ and $|H\rangle$ of Eqs. (42) and (43) to standard scalar beams using five wave plate and q -plate pairs. The first row depicts the progression of the state $|G\rangle$ and the second row depicts that of $|H\rangle$. The figure with a single line inside denotes a wave plate, whose fast-axis orientation is indicated by the orientation of this line.

VIII. CONCLUSION

In this work we have considered a bipartite quantum system comprising of a qudit degree of freedom coupled with a qubit degree of freedom. In such a composite system, we have implemented most generalized discrete-time quantum walks using position-independent coins, and then examined the set of quantum states that are accessed by such walks, starting from some easy-to-prepare product state as the initial state. A major result coming out of the current work is that such broadest generalization of the definition of quantum walks does not give access to all the states on the composite Hilbert space. A simple criterion for identifying whether a given quantum state can be accessible through a quantum walk, is provided based on the notion of translational invariance of a quantum step. Furthermore, given a walk-accessible composite state, a clear and deterministic algorithm for realizing it through discrete time quantum walks is also provided. The given construction

is “minimal” in that the given composite state cannot be obtained using fewer quantum steps of unit step size than what is given by the algorithm. To give a practical context to our theoretical results, in this paper we have interpreted them in the context of quantum walks on the spin-and-orbital angular momenta of light beams. We have demonstrated that any walk-accessible state can be generated deterministically using only wave plates and $q = \frac{1}{2} q$ plates. We believe that the results presented here will aid in designing better quantum-walk based algorithms for quantum state engineering, particularly in the linear optical implementation of discrete-time quantum walks.

APPENDIX: Γ AND α FOR THE SHRINKING ALGORITHM

Here, given a walk state $|U\rangle$ of position span $[b, e]$, we find the parameters of the quantum step $\hat{T}_\Gamma(\delta, p, s, c)$ such that the composite state $\hat{T}_\Gamma(\delta, p, s, c)|U\rangle$ has a position span of

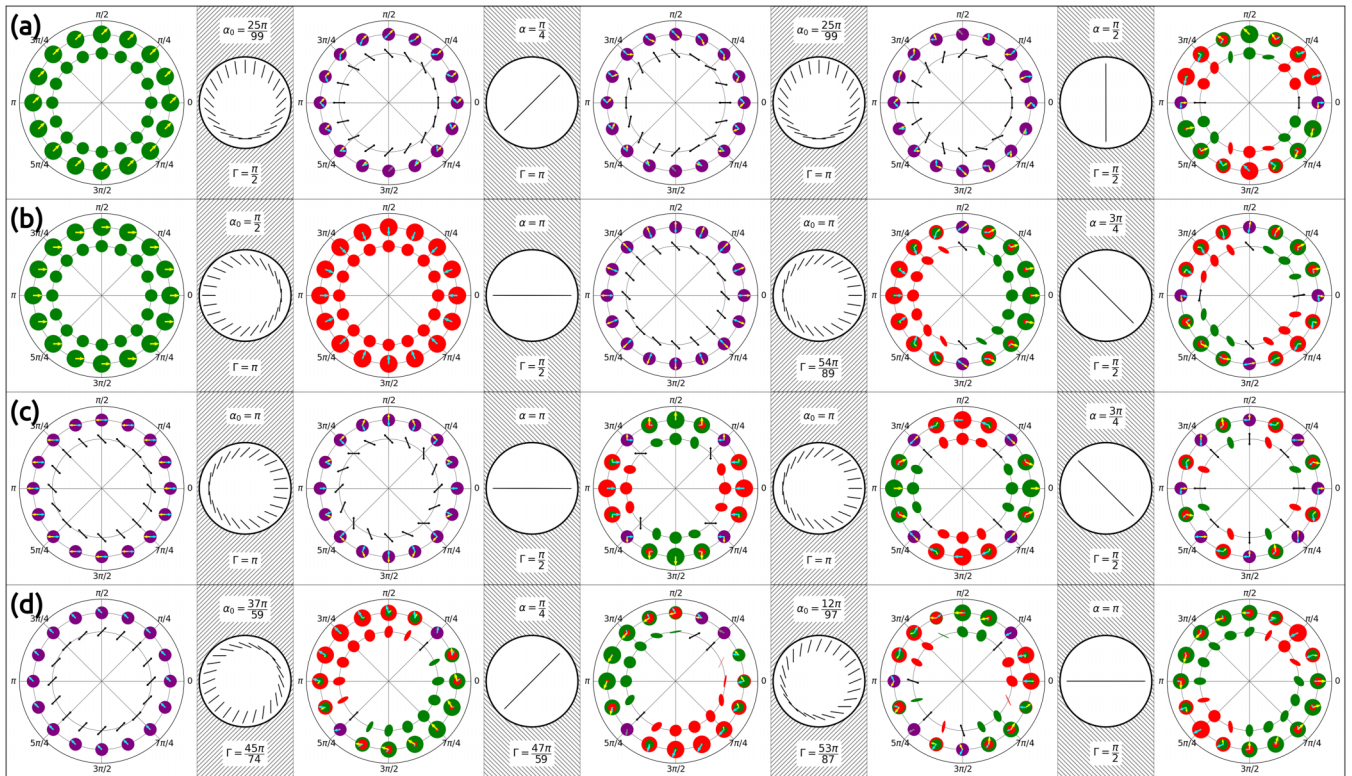


FIG. 13. Evolution of scalar beams, into each of the four-vector beams $|A\rangle$, $|B\rangle$, $|C\rangle$, and $|D\rangle$ of Eq. (41). The figure with a single line inside denotes a wave plate, whose fast-axis orientation is indicated by the orientation of this line.

$[b + 1, e - 1]$. Let $|\mathbf{R}\rangle = \hat{T}_\Gamma(\delta, p, \mathbf{s}, \mathbf{c})|U\rangle$. The composite state $|\mathbf{R}\rangle$ can be expressed in the form of Eq. (3). The amplitude at the m^{th} position r_m and the coin state there $|\mathbf{r}_m\rangle$ can be obtained by Eq. (11) as

$$r_m|\mathbf{r}_m\rangle = \left(u_m \langle \mathbf{c} | \mathbf{u}_m \rangle \cos \frac{\Gamma}{2} - u_{m+1} \langle \mathbf{c}_\perp | \mathbf{u}_{m+1} \rangle \sin \frac{\Gamma}{2} e^{-i\delta} \right) |s\rangle + \left(u_m \langle \mathbf{c}_\perp | \mathbf{u}_m \rangle \cos \frac{\Gamma}{2} + u_{m-1} \langle \mathbf{c} | \mathbf{u}_{m-1} \rangle \sin \frac{\Gamma}{2} e^{i\delta} \right) |s_\perp\rangle \quad (\text{A1})$$

We chose the parameters of $\hat{T}_\Gamma(\delta, 1, \mathbf{s}, \mathbf{c})$ such that (i) $(e + 1)^{\text{th}}$ and e^{th} positions of $|\mathbf{R}\rangle$ are unoccupied; that is, $r_{e+1} = 0$ and $r_e = 0$, and (ii) the b^{th} and $(b - 1)^{\text{th}}$ positions of $|\mathbf{R}\rangle$ are also unoccupied; that is, $r_{b-1} = 0$ and $r_b = 0$:

$$\langle \mathbf{c} | \mathbf{u}_e \rangle = 0, \quad \tan \frac{\Gamma}{2} = \frac{u_e |\langle \mathbf{c}_\perp | \mathbf{u}_e \rangle|}{u_{e-1} |\langle \mathbf{c} | \mathbf{u}_{e-1} \rangle|}, \quad \delta = \pi + \Phi(\langle \mathbf{c}_\perp | \mathbf{u}_e \rangle) - \Phi(\langle \mathbf{c} | \mathbf{u}_{e-1} \rangle). \quad (\text{A2})$$

Note that we are dealing with quantum steps of unit size, $p = 1$. The contribution to the amplitude at the $(e + 1)^{\text{th}}$ position of $|\mathbf{R}\rangle$ is therefore only from that of e^{th} position of $|U\rangle$ alone. The first condition ensures that this contribution is 0. The amplitude of e^{th} component of $|\mathbf{R}\rangle$, on the other hand, gets contributions from both e^{th} and $(e - 1)^{\text{th}}$ components of $|U\rangle$.

The chosen Γ and α of \hat{T} are such that the two contributions are equal and out of phase, so that they cancel each other.

In a similar manner, the condition that the b^{th} and $(b - 1)^{\text{th}}$ positions are unoccupied in $|\mathbf{R}\rangle$ leads to the following three conditions on the step parameters:

$$\langle \mathbf{c}_\perp | \mathbf{u}_b \rangle = 0, \quad \tan \frac{\Gamma}{2} = \frac{u_b |\langle \mathbf{c} | \mathbf{u}_b \rangle|}{u_{b+1} |\langle (\mathbf{u}_b)_\perp | \mathbf{u}_{b+1} \rangle|}, \quad \delta = \Phi(\langle \mathbf{c} | \mathbf{u}_b \rangle) - \Phi(\langle (\mathbf{u}_b)_\perp | \mathbf{u}_{b+1} \rangle). \quad (\text{A3})$$

The contribution to $(b - 1)^{\text{th}}$ of $|\mathbf{R}\rangle$ is from b^{th} component of $|U\rangle$ alone, and the first condition ensures that this contribution is 0. The b^{th} component of $|\mathbf{R}\rangle$, gets contributions from both the b^{th} and $(b - 1)^{\text{th}}$ components of $|U\rangle$ and the Γ and α of the step \hat{T} ensure that these two contributions cancel each other. The step of Eq. (A2), acting on a composite state $|U\rangle$ changes its position spread from $[b, e]$ to $[b - 1, e - 1]$ and, likewise, the step of Eq. (A3) changes the position span from $[b, e]$ to $[b + 1, e + 1]$. We are interested in shrinking the span to $[b + 1, e - 1]$, so we seek a step whose parameters satisfy both sets of constraints simultaneously. For instance, the first of Eq. (A2) and the first of Eq. (A3) can be simultaneously satisfied only if $\langle \mathbf{u}_b | \mathbf{u}_e \rangle = 0$. This is not guaranteed for any arbitrary composite state of the form Eq. (3). We, however, are not dealing with arbitrary composite states, but “walk states” satisfying Eq. (16), and for such states, it can be seen that the two set of conditions are indeed identical. We make a choice of $|\mathbf{c}\rangle = |(\mathbf{u}_e)_\perp\rangle$ so as to satisfy the first of Eqs. (A3) and (A2) simultaneously, from which Eq. (23) follows.

-
- [1] M. Kac, Random walk and the theory of Brownian motion, *Am. Math. Mon.* **54**, 369 (1947).
- [2] H. C. Berg, Random walks in biology, in *Random Walks in Biology* (Princeton University Press, Princeton, NJ, 2018).
- [3] E. A. Codling, M. J. Plank, and S. Benhamou, Random walk models in biology, *J. R. Soc., Interface* **5**, 813 (2008).
- [4] E. Scalas, The application of continuous-time random walks in finance and economics, *Physica A (Amsterdam, Neth.)* **362**, 225 (2006).
- [5] O. C. Ibe, *Elements of Random Walk and Diffusion Processes* (John Wiley & Sons, 2013).
- [6] Y. Aharonov, L. Davidovich, and N. Zagury, Quantum random walks, *Phys. Rev. A* **48**, 1687 (1993).
- [7] S. Singh, P. Chawla, A. Sarkar, and C. Chandrashekar, Universal quantum computing using single-particle discrete-time quantum walk, *Sci. Rep.* **11**, 1 (2021).
- [8] A. M. Childs, Universal Computation by Quantum Walk, *Phys. Rev. Lett.* **102**, 180501 (2009).
- [9] R. Portugal, *Quantum Walks and Search Algorithms* (Springer, 2013), Vol. 19.
- [10] V. M. Kendon, A random walk approach to quantum algorithms, *Philos. Trans. R. Soc., A* **364**, 3407 (2006).
- [11] E. Campos, S. E. Venegas-Andraca, and M. Lanzagorta, Quantum tunneling and quantum walks as algorithmic resources to solve hard K -SAT instances, *Sci. Rep.* **11**, 16845 (2021).
- [12] A. Sarkar and C. Chandrashekar, Multi-bit quantum random number generation from a single qubit quantum walk, *Sci. Rep.* **9**, 12323 (2019).
- [13] S. Panahiyan and S. Fritzsche, Toward simulation of topological phenomena with one-, two-, and three-dimensional quantum walks, *Phys. Rev. A* **103**, 012201 (2021).
- [14] S. Panahiyan and S. Fritzsche, Controllable simulation of topological phases and edge states with quantum walk, *Phys. Lett. A* **384**, 126828 (2020).
- [15] F. Cardano, M. Maffei, F. Massa, B. Piccirillo, C. De Lisio, G. De Filippis, V. Cataudella, E. Santamato, and L. Marrucci, Statistical moments of quantum-walk dynamics reveal topological quantum transitions, *Nat. Commun.* **7**, 11439 (2016).
- [16] F. Cardano, A. D’Errico, A. Dauphin, M. Maffei, B. Piccirillo, C. de Lisio, G. De Filippis, V. Cataudella, E. Santamato, L. Marrucci *et al.*, Detection of Zak phases and topological invariants in a chiral quantum walk of twisted photons, *Nat. Commun.* **8**, 15516 (2017).
- [17] S. Barkhofen, T. Nitsche, F. Elster, L. Lorz, A. Gábris, I. Jex, and C. Silberhorn, Measuring topological invariants in disordered discrete-time quantum walks, *Phys. Rev. A* **96**, 033846 (2017).
- [18] L. Innocenti, H. Majury, T. Giordani, N. Spagnolo, F. Sciarrino, M. Paternostro, and A. Ferraro, Quantum state engineering using one-dimensional discrete-time quantum walks, *Phys. Rev. A* **96**, 062326 (2017).
- [19] T. Giordani, E. Polino, S. Emiliani, A. Suprano, L. Innocenti, H. Majury, L. Marrucci, M. Paternostro, A. Ferraro, N. Spagnolo *et al.*, Experimental Engineering of Arbitrary Qudit States with Discrete-Time Quantum Walks, *Phys. Rev. Lett.* **122**, 020503 (2019).

- [20] A. Suprano, D. Zia, E. Polino, T. Giordani, L. Innocenti, A. Ferraro, M. Paternostro, N. Spagnolo, and F. Sciarrino, Dynamical learning of a photonics quantum-state engineering process, *Adv. Photonics* **3**, 066002 (2021).
- [21] A. Suprano, D. Zia, E. Polino, T. Giordani, L. Innocenti, A. Ferraro, M. Paternostro, N. Spagnolo, and F. Sciarrino, Real-time optimization of quantum state engineering protocol, in *Quantum Information and Measurement* (Optical Society of America, 2021), pp. F2C–4.
- [22] R. Zhang, R. Yang, J. Guo, C.-W. Sun, Y.-C. Liu, H. Zhou, P. Xu, Z. Xie, Y.-X. Gong, and S.-N. Zhu, Arbitrary coherent distributions in a programmable quantum walk, *Phys. Rev. Res.* **4**, 023042 (2022).
- [23] B. P. Lanyon, M. Barbieri, M. P. Almeida, T. Jennewein, T. C. Ralph, K. J. Resch, G. J. Pryde, J. L. O’Brien, A. Gilchrist, and A. G. White, Simplifying quantum logic using higher-dimensional Hilbert spaces, *Nat. Phys.* **5**, 134 (2009).
- [24] Z. Gedik, I. A. Silva, B. Çakmak, G. Karpát, E. L. G. Vidoto, D. d. O. Soares-Pinto, E. R. deAzevedo, and F. F. Fanchini, Computational speed-up with a single qudit, *Sci. Rep.* **5**, 14671 (2015).
- [25] D. Cozzolino, B. Da Lio, D. Bacco, and L. K. Oxenløwe, High-dimensional quantum communication: Benefits, progress, and future challenges, *Adv. Quantum Technol.* **2**, 1900038 (2019).
- [26] D. Kaszlikowski, P. Gnański, M. Żukowski, W. Miklaszewski, and A. Zeilinger, Violations of Local Realism by Two Entangled N -dimensional Systems are Stronger than for Two Qubits, *Phys. Rev. Lett.* **85**, 4418 (2000).
- [27] P. Rungta, W. Munro, K. Nemoto, P. Deuar, G. J. Milburn, and C. Caves, Qudit entanglement, in *Directions in Quantum Optics* (Springer, 2001), pp. 149–164.
- [28] D. Collins, N. Gisin, N. Linden, S. Massar, and S. Popescu, Bell Inequalities for Arbitrarily High-Dimensional Systems, *Phys. Rev. Lett.* **88**, 040404 (2002).
- [29] M. Schuld, I. Sinayskiy, and F. Petruccione, An introduction to quantum machine learning, *Contemp. Phys.* **56**, 172 (2015).
- [30] L. Sheridan and V. Scarani, Security proof for quantum key distribution using qudit systems, *Phys. Rev. A* **82**, 030301(R) (2010).
- [31] N. T. Islam, C. C. W. Lim, C. Cahall, J. Kim, and D. J. Gauthier, Provably secure and high-rate quantum key distribution with time-bin qudits, *Sci. Adv.* **3**, e1701491 (2017).
- [32] S. Etcheverry, G. Cañas, E. Gómez, W. Nogueira, C. Saavedra, G. Xavier, and G. Lima, Quantum key distribution session with 16-dimensional photonic states, *Sci. Rep.* **3**, 2316 (2013).
- [33] H. Bechmann-Pasquinucci and A. Peres, Quantum Cryptography with 3-State Systems, *Phys. Rev. Lett.* **85**, 3313 (2000).
- [34] T. Durt, D. Kaszlikowski, J.-L. Chen, and L. C. Kwak, Security of quantum key distributions with entangled qudits, *Phys. Rev. A* **69**, 032313 (2004).
- [35] J. Wang and K. Manouchehri, *Physical Implementation of Quantum Walks* (Springer, 2013).
- [36] C. A. Ryan, M. Laforest, J.-C. Boileau, and R. Laflamme, Experimental implementation of a discrete-time quantum random walk on an NMR quantum-information processor, *Phys. Rev. A* **72**, 062317 (2005).
- [37] J. Du, H. Li, X. Xu, M. Shi, J. Wu, X. Zhou, and R. Han, Experimental implementation of the quantum random-walk algorithm, *Phys. Rev. A* **67**, 042316 (2003).
- [38] P. Xue, B. C. Sanders, and D. Leibfried, Quantum Walk on a Line for a Trapped Ion, *Phys. Rev. Lett.* **103**, 183602 (2009).
- [39] R. Matjeschk, C. Schneider, M. Enderlein, T. Huber, H. Schmitz, J. Glueckert, and T. Schaetz, Experimental simulation and limitations of quantum walks with trapped ions, *New J. Phys.* **14**, 035012 (2012).
- [40] J.-Q. Zhou, L. Cai, Q.-P. Su, and C.-P. Yang, Protocol of a quantum walk in circuit QED, *Phys. Rev. A* **100**, 012343 (2019).
- [41] M. Karski, L. Förster, J.-M. Choi, A. Steffen, W. Alt, D. Meschede, and A. Widera, Quantum walk in position space with single optically trapped atoms, *Science* **325**, 174 (2009).
- [42] J. Boutari, A. Feizpour, S. Barz, C. Di Franco, M. Kim, W. Kolthammer, and I. Walmsley, Large scale quantum walks by means of optical fiber cavities, *J. Opt. (Bristol, U. K.)* **18**, 094007 (2016).
- [43] N. C. Harris, G. R. Steinbrecher, M. Prabhu, Y. Lahini, J. Mower, D. Bunandar, C. Chen, F. N. Wong, T. Baehr-Jones, M. Hochberg *et al.*, Quantum transport simulations in a programmable nanophotonic processor, *Nat. Photonics* **11**, 447 (2017).
- [44] A. Aspuru-Guzik and P. Walther, Photonic quantum simulators, *Nat. Phys.* **8**, 285 (2012).
- [45] P. Zhang, B.-H. Liu, R.-F. Liu, H.-R. Li, F.-L. Li, and G.-C. Guo, Implementation of one-dimensional quantum walks on spin-orbital angular momentum space of photons, *Phys. Rev. A* **81**, 052322 (2010).
- [46] S. K. Goyal, F. S. Roux, A. Forbes, and T. Konrad, Implementing Quantum Walks Using Orbital Angular Momentum of Classical Light, *Phys. Rev. Lett.* **110**, 263602 (2013).
- [47] B. Sephton, A. Dudley, G. Ruffato, F. Romanato, L. Marrucci, M. Padgett, S. Goyal, F. Roux, T. Konrad, and A. Forbes, A versatile quantum walk resonator with bright classical light, *PLoS One* **14**, e0214891 (2019).
- [48] R. Dorn, S. Quabis, and G. Leuchs, Sharper Focus for a Radially Polarized Light Beam, *Phys. Rev. Lett.* **91**, 233901 (2003).
- [49] B. Sick, B. Hecht, and L. Novotny, Orientational Imaging of Single Molecules by Annular Illumination, *Phys. Rev. Lett.* **85**, 4482 (2000).
- [50] Q. Zhan, Cylindrical vector beams: From mathematical concepts to applications, *Adv. Opt. Photonics* **1**, 1 (2009).
- [51] M. Woerdemann, C. Alpmann, M. Esseling, and C. Denz, Advanced optical trapping by complex beam shaping, *Laser Photonics Rev.* **7**, 839 (2013).
- [52] C. Rosales-Guzmán, B. Ndagano, and A. Forbes, A review of complex vector light fields and their applications, *J. Opt. (Bristol, U. K.)* **20**, 123001 (2018).
- [53] Y. Yang, Y. Ren, M. Chen, Y. Arita, and C. Rosales-Guzmán, Optical trapping with structured light: A review, *Adv. Photonics* **3**, 034001 (2021).
- [54] A. Ekert and P. L. Knight, Entangled quantum systems and the schmidt decomposition, *Am. J. Phys.* **63**, 415 (1995).
- [55] A. Pathak, *Elements of Quantum Computation and Quantum Communication* (CRC Press, Boca Raton, 2013).
- [56] C. M. Chandrashekar, R. Srikanth, and R. Laflamme, Optimizing the discrete time quantum walk using a SU(2) coin, *Phys. Rev. A* **77**, 032326 (2008).
- [57] M. Montero, Unidirectional quantum walks: Evolution and exit times, *Phys. Rev. A* **88**, 012333 (2013).

- [58] M. Montero, Quantum walk with a general coin: Exact solution and asymptotic properties, *Quantum Inf. Process.* **14**, 839 (2015).
- [59] A. Suzuki, Asymptotic velocity of a position-dependent quantum walk, *Quantum Inf. Process.* **15**, 103 (2016).
- [60] S. Panahiyan and S. Fritzsche, Controlling quantum random walk with a step-dependent coin, *New J. Phys.* **20**, 083028 (2018).
- [61] A. P. Flitney, D. Abbott, and N. F. Johnson, Quantum walks with history dependence, *J. Phys. A: Math. Gen.* **37**, 7581 (2004).
- [62] P. P. Rohde, G. K. Brennen, and A. Gilchrist, Quantum walks with memory provided by recycled coins and a memory of the coin-flip history, *Phys. Rev. A* **87**, 052302 (2013).
- [63] G. Di Molfetta, D. O. Soares-Pinto, and S. M. D. Queirós, Elephant quantum walk, *Phys. Rev. A* **97**, 062112 (2018).
- [64] F. Cardano, F. Massa, H. Qassim, E. Karimi, S. Slussarenko, D. Paparo, C. de Lisio, F. Sciarrino, E. Santamato, R. W. Boyd *et al.*, Quantum walks and wavepacket dynamics on a lattice with twisted photons, *Sci. Adv.* **1**, e1500087 (2015).
- [65] R. Simon and N. Mukunda, Universal SU(2) gadget for polarization optics, *Phys. Lett. A* **138**, 474 (1989).
- [66] R. Simon and N. Mukunda, Minimal three-component SU(2) gadget for polarization optics, *Phys. Lett. A* **143**, 165 (1990).
- [67] S. Liu, P. Li, T. Peng, and J. Zhao, Generation of arbitrary spatially variant polarization beams with a trapezoid Sagnac interferometer, *Opt. Express* **20**, 21715 (2012).
- [68] P. Li, Y. Zhang, S. Liu, C. Ma, L. Han, H. Cheng, and J. Zhao, Generation of perfect vectorial vortex beams, *Opt. Lett.* **41**, 2205 (2016).
- [69] C. Rosales-Guzmán, N. Bhebhe, and A. Forbes, Simultaneous generation of multiple vector beams on a single SLM, *Opt. Express* **25**, 25697 (2017).
- [70] Z. Chen, T. Zeng, B. Qian, and J. Ding, Complete shaping of optical vector beams, *Opt. Express* **23**, 17701 (2015).
- [71] Y. Gao, Z. Chen, J. Ding, and H.-T. Wang, Single ultra-high-definition spatial light modulator enabling highly efficient generation of fully structured vector beams, *Appl. Opt.* **58**, 6591 (2019).
- [72] P. García-Martínez, D. Marco, J. L. Martínez-Fuentes, M. del Mar Sánchez-López, and I. Moreno, Efficient on-axis slm engineering of optical vector modes, *Opt. Lasers Eng.* **125**, 105859 (2020).
- [73] A. Rubano, F. Cardano, B. Piccirillo, and L. Marrucci, Q-plate technology: A progress review, *J. Opt. Soc. Am. B* **36**, D70 (2019a)..
- [74] G. Kadiri, G. Raghavan, and G. Raghavan, Wavelength-adaptable effective q-plates with passively tunable retardance, *Sci. Rep.* **9**, 11911 (2019).
- [75] B. Piccirillo, V. D'Ambrosio, S. Slussarenko, L. Marrucci, and E. Santamato, Photon spin-to-orbital angular momentum conversion via an electrically tunable q-plate, *Appl. Phys. Lett.* **97**, 241104 (2010).
- [76] V. D'Ambrosio, F. Baccari, S. Slussarenko, L. Marrucci, and F. Sciarrino, Arbitrary, direct and deterministic manipulation of vector beams via electrically-tuned q-plates, *Sci. Rep.* **5**, 7840 (2015).
- [77] Arcoptix, Switzerland, http://www.arcoptix.com/radial_polarization_converter.htm, [Accessed: 5-May-2022].
- [78] M. Born and E. Wolf, *Principles of Optics: Electromagnetic Theory of Propagation, Interference and Diffraction of Light* (Elsevier, 2013).
- [79] S. Delaney, M. M. Sánchez-López, I. Moreno, and J. A. Davis, Arithmetic with q-plates, *Appl. Opt.* **56**, 596 (2017).
- [80] M. J. Padgett and J. Courtial, Poincaré-sphere equivalent for light beams containing orbital angular momentum, *Opt. Lett.* **24**, 430 (1999).
- [81] G. Milione, H. I. Sztul, D. A. Nolan, and R. R. Alfano, Higher-Order Poincaré Sphere, Stokes Parameters, and the Angular Momentum of Light, *Phys. Rev. Lett.* **107**, 053601 (2011).
- [82] E. Collett, *Polarized Light in Fiber Optics* (SPIE Press, 2003).